http://researchcommons.waikato.ac.nz/

Research Commons at the University of Waikato

Copyright Statement:

The digital copy of this thesis is protected by the Copyright Act 1994 (New Zealand).

The thesis may be consulted by you, provided you comply with the provisions of the Act and the following conditions of use:

- Any use you make of these documents or images must be for research or private study purposes only, and you may not make them available to any other person.
- Authors control the copyright of their thesis. You will recognise the author's right to be identified as the author of the thesis, and due acknowledgement will be made to the author where appropriate.
- You will obtain the author's permission before publishing any material from the thesis.

Fabrication of advanced heat sink materials by powder metallurgy approach

A thesis submitted in fulfilment

of the requirements for the degree

of

Master of Engineering in Materials and Processing Engineering

at

The University of Waikato

by

Yaqi Chang

Supervised by Dr. Fei Yang

2021

Abstract

To guarantee a safe work environment for high-end chips, electronic packaging materials should have high thermal conductivity, matched coefficient of thermal expansion to semiconductor, low density, good impact toughness, and tensile strength. Diamond/graphite flakes-reinforced composites are considered as the new generation of heat sink material, however, the poor chemical affinity between copper and diamond and between copper and graphite flakes hinder the composites from achieving high thermal conductivity. The interface between copper matrix and diamond reinforcement or graphite flakes reinforcement is the key factor for improving heat transfer of the composites.

This study aims to investigate the mechanisms of how the interface improves the thermal conductivity of the diamond/graphite flakes-reinforced composites. The primary research includes: (1) study the effect of vacuum sintering process on the formation of carbide layer; (2) investigate the effect of the volume fraction of diamond particles on relative density and thermal conductivity of the copper/diamond composites, and (3) explore the feasibility to fabricate graphite flakes reinforced copper composites by powder forging and investigate the effect of graphite flakes' volume fraction on the thermal conductivity of the fabricated composites.

Tungsten carbide (WC) can be formed during the vacuum sintering process, however, the formed WC were broken during the subsequent 1050 ℃ hot forging process. The WC can be formed during the vacuum sintering process above 550 ℃ for 30mins, on both diamond -{100}facet and -{111}facet. Cu-55WDia-1050HF has a thermal conductivity of 230.5W/(mK) which is higher than Cu-55WDia-VS800C2h-1050 of 195.1W/(mK). With the volume fraction of diamond from 45vol% to 65vol%, the thermal conductivity reduced from 250.8 to 65.1W/(mK).

For copper/graphite flakes composites, the addition of carbide forming element Ti helped to improve the thermal conductivity. Because of the excessive copper fluidity in Cu-Ti-50GFs-1050HF, Cu-Ti-50GFs-1050HF has the lower thermal conductivity of 202.7 W/(mK) than thermal conductivity of Cu-Ti-50GFs-950HF which is 375.0 W/(mK). With the volume fraction of the graphite flakes from 30% to 70%, the relative density changed from 100% to 83.3%.

Acknowledgment

This study was completed under the supervision of Dr. Fei Yang. He helped me to improve my research and academic writing. The encouragement he brought me is endless. Sincerely thank you for your help in topic supporting. His rigorous scientific research spirit will affect me in the future and my life.

I need to thank all of the members of the research group, Jingnan Ma and Yutao Zhai helped me a lot with the operation of the experiment. Jingnan Ma also helped me a lot with the research experience. I have finished my master's study successfully because of their help.

Thanks also go to Shanquan Jia under the supervision of Dr. Fei Yang, for helping with his thoughtful discussion.

Sincere thanks to my parents, they support me a lot when I feel down. Even though we are separated from each other in different countries, they are still concentrated about my life and study. Their financial support and their understanding ensured my master's study can do smoothly and can be finished.

Thanks to my friends, Jingnan Ma, Yulu Sun, and Xinhan Zhang, for accompanying me in my master's life, we encourage each other and helped each other, make life more interesting and exciting, we have a sincere friendship.

My thanks to many others who I could not specify directly.

Table of contents

Abstract I

Acknowledgments III

Table of contents III

List of symbols VII

List of Figures VIII

List of Tables X

List of Abbreviations XI

1 Introduction 2

2 Literature review 4

2.1 Heat sink material 4

2.2 Common materials as reinforcement 8

2.2.1 Diamond 8

2.2.2 Graphite flakes 11

2.3 Method for modifying interface 14

2.3.1 Metal matrix alloying 14

2.3.2 Diamond surface metallization 15

2.4 Fabrication of composites 17

2.4.1 Vacuum hot pressing (VHP) 17

2.4.2 Spark plasma sintering (SPS) 18

2.4.3 Electrodeposition 20

2.4.4 Powder hot forging 22

2.5 Summary and Research objectives 23

3 Experimental Procedure 25

3.1 Materials Preparation 25

3.1.1 Raw Materials 25

3.1.1.1 Copper 25

3.1.1.2 Diamond particles 25

3.1.1.3 Graphite flakes 25

3.1.2 Cleaning of raw materials 25

3.2 Manufacturing Process 26
3.2.1 Mixing of raw materials 26
3.2.2 Compaction 26
3.2.3 Vacuum sintering 26
3.2.4 Hot forging 26
3.3 Property testing 28
3.3.1 Density 28
3.3.2 Microstructure 28
3.3.3 Phase constitution 29
3.3.4 Thermal diffusivity 30
3.3.5 Thermal conductivity 30
4 Cu/diamond composites 31
4.1 Effect of vacuum sintering on Cu/diamond composites 31
4.1.1 Relative density 31
4.1.2 Phase constitutions 32
4.1.3 Microstructure 34
4.1.4 Thermal conductivity 38
4.1.5 Discussion 38
4.1.5.1 Effect of vacuum sintering process on relative density and microstructure 38
4.1.5.2 Effect of vacuum sintering process on thermal conductivity 40
4.1.5.3 Effect of vacuum sintering on formation of interface 41
4.2 Effect of volume fraction of diamond particles on Cu/Dimond composites 41
4.2.1 Relative density 42
4.2.2 Phase constitutions 42
4.2.3 Microstructure 44
4.2.4 Thermal conductivity 45
4.2.5 Discussion 46
4.2.5.1 Effect of the volume fraction of diamond particles on relative

density and microstructure 46
4.2.5.2 Effect of volume fraction of diamond particles on thermal conductivity 47
4.3 Summary 48
5 Cu/Graphite flakes composites 49
5.1 Relative density 51
5.2 Phase constitutions 51
5.3 Microstructure 52
5.4 Thermal conductivity 55
5.5 Discussion 56
5.5.1 Effect of volume fraction of graphite flakes 56
5.5.2 The effect of hot forging temperature on thermal conductivity GFs/copper composites 57
5.5.3 The effect of Ti powder on interface of Cu/ graphite flakes composites 58
5.6 Summary 58
6 Conclusion 60
Reference 61

List of symbols

λ (W/mK)	Thermal Conductivity of the composites
α (m^2 /s)	Thermal Diffusivity
ρ (kg/m^3)	Density of the composite

List of Figures

Figure 2-1 Diamond structure [9] 9
Figure 2-2 Graphite structure [13] 12
Figure 2-3 Alignment structure of graphite flakes in matrix [14] 13
Figure 2-4 Schematic diagram of vacuum hot pressing process [26] 18
Figure 2-5 Schematic diagram of spark plasma sintering [29] 19
Figure 2-6 Schematic diagram of electrodeposition [22] 21
Figure 2-7 Schematic diagram of hot forging [35] 22
Figure 3-1 Image of SEM, HITACHI, s4700. 29
Figure 3-2 Image of XRD, Philips 29
Figure 4-1 Relative density of Cu-55WDia-1050HF and Cu-55WDia-VS800/2h-1050HF 32
Figure 4-2 Phase constitution of: (a) Cu-55WDia-VS800C2h, (b) Cu-55WDia-VS800C2h-1050HF, and (c) Cu-55WDia-1050HF 33
Figure 4-3 Microstructure of Cu-55WDia-VS800C2h-1050HF(a-c), and Cu-55WDia-1050HF(d-e) 35
Figure 4-4 Extracted diamond particles from Cu-55WDia-VS800C2h-1050HF(a-c); Cu-55-Dia-1050HF(d-f). 36
Figure 4-5 Extracted diamond particles of Cu-55WDia-1050HF 36
Figure 4-6 Thermal diffusivity and thermal conductivity of Cu-WDia-VS800C2h-1050HF, and Cu-W-Dia-1050HF 38
Figure 4-7 Relative density of Cu-45WDia-1050HF, Cu-55WDia-1050HF, and Cu-65WDia-1050HF 42
Figure 4-8 The phase constitution of: (a)Cu-65WDia-1050HF, (b)Cu-55WDia-1050HF, and (c)Cu-45WDia-1050HF 43
Figure 4-9 Microstructure of (a-c) Cu-45WDia-1050HF, (d-e) Cu-55WDia-1050HF, and (g)-(i) Cu-65WDia-1050HF 44
Figure 4-10 Microstructure of the extracted diamond particles from (a-c) Cu-45WDia-1050HF, (d-e) Cu-55WDia-1050HF, and (g)-(i) Cu-65WDia-1050HF composites 45

Figure 4-11 Thermal diffusivity and thermal conductivity of Cu-45WDia-1050HF, Cu-55WDia-1050HF, and Cu-65WDia-1050HF composites 46
Figure 5-1 The processing of fabricating the Cu/graphite flakes composites..... 49
Figure 5-2 Relative density of Cu/Graphite flakes composites 51
Figure 5-3 The X-ray diffraction patterns of: (a)Cu-Ti-50GFs-950HF, (b)Cu-Ti-70GFs-1050HF, (c)Cu-Ti-60GFs-1050HF, (d)Cu-Ti-50GFs-1050HF, (e)Cu-Ti-40GFs-1050HF, and (f)Cu-Ti-30GFs-1050HF 52
Figure 5-4 Microstructure of Cu-Ti-50GFs-1050HF(a)-(d); Cu-Ti-50GFs-950HF(e)-(h) in the direction parallel to stress 53
Figure 5-5 Microstructure of the extracted graphite flakes of Cu-Ti-30GFs-1050HF(a)-(c), Cu-Ti-40GFs-1050HF(d)-(f), Cu-Ti-50GFs-1050HF(g)-(i), Cu-Ti-60GFs-1050HF(j)-(l), Cu-Ti-70GFs-1050HF(m)-(o), and Cu-Ti-50GFs-950HF(p)-(r)..... 54
Figure 5-6 Thermal conductivity of Cu-Ti-50GFs-950HF along the direction to the applying force and Cu-Ti-50GFs-950HF along the direction perpendicular to the applying force..... 56

List of Tables

Table 2-1 Properties of diamond [10] 10

Table 3-1 Fabricated copper/Diamond composites..... 27

Table 3-2 Fabricated copper/Graphite flakes composites 28

Table 4-1 Composites to investigate the effect of vacuum sintering on Cu/diamond composites..... 31

Table 4-4 Composites to investigate the volume fraction of diamond..... 41

Table 5-1 Cu/graphite flakes composites 50

List of Abbreviations

CTE	Coefficient of Thermal Expansion
SEM	Scanning Electron Microscopy
TC	Thermal Conductivity
XRD	X-ray Diffraction

1 Introduction

With the development of information technology, the electronics manufacturing industry has become a pillar industry. In the new period of science and technology development, high-end chips and very large-scale integrated circuit manufacturing are major projects. The complicated functions of electronic devices and the integration of electronic devices is getting higher and higher, the size is continuously decreasing, and the heat flux density is greatly increased. To satisfy the requirements, the ideal electronic packaging material should meet the following performance requirements : (1) Thermal conductivity (TC) > 400 W/(mK) to ensure that the heat can be dissipated in time when the electronic device is working normally; (2) Coefficient of thermal expansion (CTE) must be matched with the semiconductor chip, 4×10^{-6} ～ 7×10^{-6} K^{-1} to avoid thermal stress damage during heating in the process caused by the mismatch of the heat sink material and the chip; (3) low density; (4) comprehensive mechanical properties such as good tensile strength and impact toughness: packaging materials must provide support protection to electronic components.

Diamond has the highest thermal conductivity among the substance in nature, it is about (1800-2200 W/(mK)); it also has a low coefficient of thermal expansion (CTE), it is about 1.5×10^{-6}-4.8×10^{-6}/K. Graphite flakes have the in-plane thermal conductivity of 500-1900 W/ (mK) and the through-plane thermal conductivity of 10-20 W/ (mK), thus graphite flakes have unique anisotropic thermal property. Copper has the second highest thermal conductivity (398 W/ (mK)) among metal, second only to Ag's 427 W/ (mK). However, it is much cheaper than Ag, and the copper's coefficient of thermal expansion is 17.5×10^{-6} K^{-1}, lower than that of Ag and Al. The superior thermal conductivity and adjustable CTE of diamond, graphite flakes and copper can meet the special applications in the thermal management field. However, the chemical affinity between the copper and the diamond and the copper and the graphite flakes is poor, it causes a high thermal resistance between copper and diamond and copper and graphite flakes. It reported that the interface failure is

the main reason causing the composites having a low thermal conductivity [1]. To improve the thermal conductivity of diamond/graphite flakes reinforced copper matrix composites, a carbide needs to be formed between the copper and the and the reinforcement of diamond/graphite flakes [2]. To improve the interfacial bonding between the copper matrix and the reinforcement of diamond/graphite flakes, matrix alloying and diamond surface metallization can be used. Common elements being used are W, Ti, B and Cr etc. At present, the study of knowing how to form and optimize the effective interface still needs a deeper researching because of the improving of thermal conductivity.

In this study, Cu/55vol% tungsten coated diamond composites are fabricated by vacuum sintering at 800℃ for 2 hours, 1hour and 30mins; 750℃ for 1 hour and 30mins; 650℃ for 30mins and 550℃ for 30mins to investigate the effect of vacuum sintering process on thermal conductivity of the copper/diamond composites. Cu/30vol%-70vol% graphite flakes mixed with Ti powder are fabricated by hot forging to investigate the effect of volume fraction of the graphite flakes on thermal conductivity of copper/graphite flakes composites.

2 Literature review

2.1 Heat sink material

Since the 21st century, mankind has entered the era of comprehensive information. With the development of integrated circuit and electronic packaging technology, the total power density of electronic components continues to grow. However, the physical size of electronic components and electronic equipment gradually tends to be miniaturized, and the heat generated rapidly accumulates. Integrated devices are at risk of stability and safety due to the rapid increase in the surrounding heat flux density. To guarantee the electronic devices work effectively, safely and stably, the research and development of electronic packaging heat dissipation materials with stable, excellent thermal conductivity and good mechanical properties have become the top priority of the modern microelectronics industry information.

In microelectronic packaging technology, the electronic packaging material is an important part. It is a matrix material with good electrical insulation, which plays the role of carrying electronic components and their interconnections, mechanical support, sealing and environmental protection, and dissipating heat of electronic components. To guarantee the electronic devices have a good packaging effect and work stably, the electronic packaging materials are required to have the following properties:

(1) **Excellent thermal conductivity**. When electronic components work, the consumed electrical energy is converted into heat energy, and the heat accumulation makes the temperature of the electronic components rise. With every 18K-increase in the working temperature, the failure probability will increase by 2-3 times. Therefore, to ensure the safe operation of electronic components, packaging materials are required to dissipate heat in a short time.

(2) **Suitable coefficient of thermal expansion**. The electronic packaging

material should have a coefficient of thermal expansion that matches the chip material such as silicon, gallium arsenide, and Indium Phosphide. This is because electronic components usually work in an environment where the temperature is constantly changing, and the shrinkage and expansion of the material will change with the change of temperature. The matched coefficient of thermal expansion can avoid the thermal stress between the interface or the structure caused by the difference in the size of the material, and ensure the packaging Effective coordination of materials and electronic components during work.

(3) **Good mechanical properties**. To better support and protect electronic components, electronic packaging materials must have good mechanical properties such as good tensile strength and hardness.

(4) **Low density**. Portable electronic devices or electronic equipment in the aerospace field have the characteristics of miniaturization and portability, so the corresponding electronic packaging materials should have a low density to reduce the weight of the device.

(5) **Good air tightness**. Normally, electronic components work in a dust-free or vacuum environment. Electronic packaging materials are required to have the extremely high density to protect electronic components from interference such as moisture and dust. In recent years, as electronic components are gradually used in hostile environments such as high temperature, high humidity, corrosion, pollution, radiation, light, and interfering electrical signals, higher requirements have been placed on the density of electronic packaging materials to protect electronic components can withstand the impact of harmful environments.

Development of heat dissipation materials for electronic packaging

Electronic packaging heat dissipation materials are divided into three categories: plastic, ceramic, and metal.

Plastic package heat dissipation materials are mainly thermosetting plastics, including phenolic, epoxy, polyester, and silicone polymer materials, among which epoxy resin is the most widely used material. Because plastic packaging materials have the advantages of low density, good insulation performance, impact resistance, low price, simple process, etc., they are suitable for mass production and application. However, plastic packaging materials have obvious defects, such as poor airtightness, and it is difficult to prevent the penetration of moisture in the air into the packaged device. These defects cause corrosion damage to the internal metal layer of the packaged device and reduce the thermodynamic properties of the material, eventually causing rapid failure of packaged devices. In addition, the low thermal conductivity, high coefficient of thermal expansion, and poor thermal cycle performance of plastic packaging materials make it difficult for materials to meet the thermal physical performance requirements of the current heat sink materials.

To overcome the shortcomings of plastic electronic packaging heat dissipation materials, ceramic packaging heat dissipation materials with good moisture resistance, insulation, and chemical stability, and good coefficient of thermal expansion and thermal conductivity have been developed and applied for practical industrial production. The most widely used ceramic heat sink material is Al_2O_3. However, due to the relatively high preparation temperature of the ceramic heat sink materials, the difficult molding process and the high cost, and the difficulty of mass production, this will inevitably limit its large-scale application in large-scale integrated circuits. Currently, it is mostly used for advanced sealed chips packages.

Compared with plastic and ceramic electronic packaging heat dissipation materials, metal packaging heat dissipation materials have the advantages of higher thermal conductivity, and acceptable strength and processability, etc. [3], the research started earlier and is widely used in power devices. Initially, researchers found that traditional metals such as Ag, Cu, and Al. have high thermal conductivity due to the large amount of free electrons involved in heat conduction, and are widely used in

high-power device housings, electronic component bases, and heat sink materials. However, these metal materials have a relatively high coefficient of thermal expansion, and mismatch to the electronic components. When the chip is working, the coefficient of thermal expansion of the chip is too different from that of the base, which causes large thermal stress. As a result, the packaging system is destroyed and the overall reliability of electronic devices is reduced.

To overcome the shortcomings of the mismatch of the coefficient of thermal expansion between traditional metal packaging materials and chips, researchers developed Kovar alloy and Invar alloy [4] through the alloy design method, which is called the first generation of electronic packaging heat dissipation materials. Although the coefficient of thermal expansion of Invar alloy and Kovar alloy can match with the chips, the alloy is prepared by adding Ni and Co, the cost is high and the thermal conductivity is low. Composite materials are considered to be the new heat sink material. Composites have multi-phase and they are prepared by at least two kinds of materials through the fabrication process. In composites, the matrix and the reinforcement collectively affect the properties of the composite, the comprehensive performance is better than the component materials of the composite. Metal matrix composites reinforced by other materials with high thermal conductivity are considered as new heat sink material. The performance of the composites is changeable. To obtain the ideal property, the composite should have: (1) metal matrix with high thermal conductivity;(2) formability thus the composite can be achieved by proper fabrication process; (3) high thermal conductivity and suitable coefficient of thermal expansion.

For metal matrix composite materials, copper and aluminum are commonly used matrix because of their high thermal conductivity, and the reinforcements include diamond, graphene [5], carbon nanotubes [6], and graphite flakes [7] because they have high thermal conductivity. Among them, diamond has the highest thermal conductivity in nature and graphite flakes have extremely high thermal conductivity

along the plane. Besides, diamond has a low coefficient of thermal expansion, low density, and isotropic thermophysical properties. Graphite flakes have a low coefficient of thermal expansion, low density and are cost-effective. Thus, diamond and graphite flakes are considered as the reinforcement for metal matrix composites.

2.2 Common materials as reinforcement

2.2.1 Diamond

Diamond is a mineral composed of pure carbon, and it is also the hardest and highest thermal conductivity substance in nature. As shown in Figure 2-1, a diamond is a crystal structure composed of two face-centered cubic lattices. One carbon atom moving 1/4 of the diagonal length along the diagonal of the unit cell cubic structure and contains four atoms in one face-centered cubic cell which are located at 1/4 of the four diagonals. These four nearest carbon atoms are on the top corners of the regular tetrahedron and are connected by covalent bonds. The atomic arrangement belongs to the plane-centered cubic Bravais lattice. At present, the artificial single-crystal diamond particles produced in the industry are mostly hexagon-octahedral.

Both diamond and graphite are allotropes of carbon. The difference lies in the arrangement of the carbon atoms. The carbon atoms in diamonds are arranged in a regular tetrahedron. Each unit cell of diamond has eight carbon atoms, each carbon atom has four nearest neighbors and twelve next-adjacent atoms, and the distance between the nearest atoms is 0.154nm. Each carbon atom forms a covalent bond with the other 4 adjacent carbon atoms through SP^3 hybridization. The C-C bond in diamond has a strong covalent bonding. There are no free electrons between the crystals, and it has a face-centered cubic structure. The surface energy of diamond -{111}and diamond -{100} facets are 5×10^{-5} J/cm^2 and 8×10^{-5} J/cm^2 [8].
The relatively low surface energy of diamond -{100}facets causes the atoms on the diamond -{111} facets less active than the atoms on diamond -{100} facets.

Figure 2-1 Diamond structure [9]

The characteristics of covalent bonds and directionality between carbon atoms in the crystal structure of diamond make diamond have a very stable crystal structure. The stable crystal structure helps diamond has good mechanical properties and good thermo-physical properties.

For example, (1) The Young's modulus is extremely high: The Young's modulus of a diamond is about 1100GPa; (2) The thermal conductivity is very high: Diamond is the material with the highest thermal conductivity in nature. According to diamond doped with nitrogen and boron, the content of elements divides diamonds into two types, type I and type II. The thermal conductivity of type II natural diamond is 2000 W/(mK), and the thermal conductivity of synthetic diamond can reach 1900 W/(mK), even exceeding that of type II. The thermal conductivity of the isotopic purity (C12 is 99.9 %) synthetic single-crystal diamond can reach 3300 W/(mK); (3) The resistivity is very high: the resistivity of a diamond is greater than 1011 Ω cm; (4) The coefficient of thermal expansion is very low: the coefficient of thermal expansion of diamond is 0.8×10^{-6}/K to 2.3 $\times10^{-6}$/K. It is precise because

the diamond has high thermal conductivity, low coefficient of thermal expansion, and excellent mechanical properties, diamond particle reinforced metal matrix composites should theoretically have high thermal conductivity and low coefficient of thermal expansion and are expected to become a new generation of high-performance electronics package heat dissipation material.

Since diamond has a high thermal conductivity (500-2000 W/(mK)) which significantly exceeds that of Cu, approximately 400 (W/mK), and a low coefficient of thermal expansion, making it a reinforcement material. The properties of the diamond are shown in Table 2-1.

Table 2-1 Properties of diamond [10]

Density (g/cm^3)	3.52	Fracture toughness ($MPa*m^{1/2}$)	3.4
Hardness (GPa)	50-100	Coefficient of thermal expansion ($10^{-6}/K$)	0.8-2.3
Compressive strength (GPa)	9	Poisson's ratio	0.07
Thermal conductivity (W/mK)	600-2000	Tensile strength (MPa)	1050-3000
Young's modulus (GPa)	1000-1100		

Zhongnan [11] used Cr as an additional element to improve the interface between diamond reinforcement and copper matrix, with Cr content increasing from 0.3-1.0 wt%, the thermal conductivity of the Diamond/Cu-Cr composite increases from 452 W/mK to 696 W/mK and then decreases from 696 W/mK to 540 W/mK. The maximum thermal conductivity of 696 W/mK was obtained at 0.5wt% Cr addition. The interface structure evolves from the discontinuous point contact to continuous strip carbides depending on the availability of Cr content.

Qiping [12] fabricated copper-diamond composite by vacuum pressure infiltration and investigated the effect of tungsten carbide. The WC coating was synthesized on diamond particle surfaces using the molten salt method, and the WC coating was formed uniformly on the diamond particles when the composite was sintered at 1050°C for 60 min. The WC coating can significantly raise the density of the copper-diamond composites from 97.5% to 99.5%, and this is because WC coating can improve the interfacial bonding between the diamond particles and copper matrix and facilitate the densification of overall composites.

2.2.2 Graphite flakes

For graphite flakes (as shown in Figure 2-2), the carbon atoms in graphite are arranged in hexagonal layers and have a layered planar structure. The carbon atoms in each layer are arranged in a honeycomb crystal structure. The atoms spacing at the layer is 0.142nm and the layer spacing is 0.335nm. Each carbon atom in the layer forms a ternary coordinated SP^2 hybrid that is covalently connected to the other 3 carbon atoms and is arranged in honeycomb-like multiple hexagons, with weak van der Waals force, and graphite has a hexagonal crystal structure.

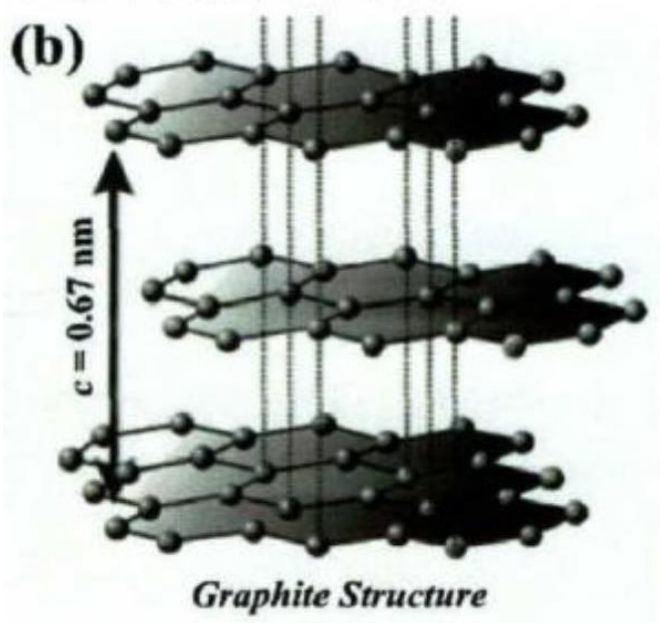

Figure 2-2 Graphite structure [13]

Natural graphite flakes composed of up to 98% crystalline graphite, and they are very soft and good conductors of electricity and heat. Its remarkable layered structure leads to obvious anisotropy of its physical properties, including electrical and thermal conductivity and coefficient of thermal expansion. Graphite flakes are multilayer graphite structures composed of thin layers of carbon atoms through weak van der Waals forces. The anisotropy of the structure leads to the anisotropy of the performance of flake graphite. There is an ultra-high thermal conductivity along the direction of the graphite layer, and the direction of the vertical layer is relatively high. With high and low thermal conductivity in a different directions, it can be used as a heat sink and thermal insulation material at the same time and used in electronic components to eliminate local hot spots.

The flake shape of graphite offers it alignment structure, as shown in Figure 2-3.

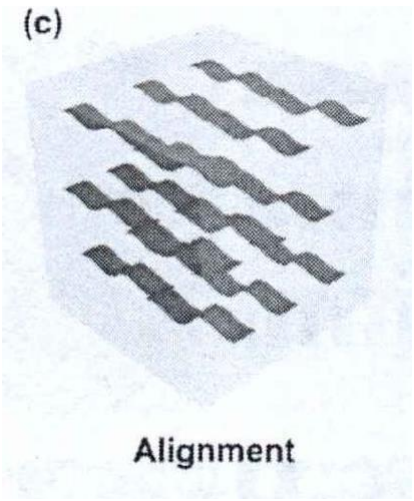

Figure 2-3 Alignment structure of graphite flakes in matrix [14]

Ankit [7] successfully prepared composites with varying content of TiC particles in copper/graphite flakes through the flake powder metallurgy process. It shows that the sintered density of the composites decreases with the addition of the TiC particles. It is because when TiC content increasing, the porosity is increasing and hence low density.

Liu [15] fabricated graphite flakes/copper composites with different equivalent particles sizes of graphite flakes from 62μm to 292μm via the vacuum hot pressing process with in-plane thermal conductivity reaching 612 W/(mK).

Zhao [16] investigated the effect of the additional element boron, boron powder of 0.4wt% adding significantly increased the thermal conductivity of 50vol% graphite flakes/copper composite from 563.00 W/(mK) to 634.87 W/(mK). It shows that the addition of boron is conducive for the copper matrix to spread on the rough graphite flakes surface and thus filling the gaps and microvoids caused by the insufficient filling of the copper matrix.

Ren [17] prepared graphite flakes/copper composites successfully by vacuum hot pressing. The study shows the formation of a carbide layer at the graphite/copper

interface can markedly improve the thermal conductivity, coefficient of thermal expansion, and bending strength of the composite, and provides a simple method to improve the properties of graphite flakes/copper composites.

2.3 Method for modifying interface

From the previous section, it has been known that copper and diamond or copper and graphite flakes have a poor chemical affinity which can cause poor interfacial bonding, thus leading to the composites have low thermal conductivity and poor chemical properties. To improve the interfacial bonding strength, carbide forming elements have to be added, the common approaches are: (1) metal matrix alloying, (2) diamond and graphite flakes surface metallization.

2.3.1 Metal matrix alloying

Metal matrix alloying can be achieved through adding alloy elements into the metal matrix, the additive element should be a carbide forming element, and the formed metal carbide can improve the chemical affinity and also inhibit the reaction between copper matrix and diamond or copper matrix and graphite flakes at the interface. This method is easy to operate, relatively cost-effective, and effectively improving thermal conductivity. However, the additive elements can form a solid solution and decrease the thermal conductivity of the metal matrix thus decrease the thermal conductivity of the composite.

Bai [18] prepared Cu-B/diamond composite by gas pressure infiltration. The boron used was boron particles (size 3-8mm), the Cu-0.3wt%B/diamond composite has a thermal conductivity of 868 W/(mK). Bai indicated that the formation of interfacial boron carbide was critical to the enhancement of thermal conductivity of the Cu-B/diamond composites.

Chu [19] prepared Cu-Zr/diamond composites by hot pressing sintering, the Cu-

1.2wt%Zr/diamond composites have a thermal conductivity of 615 W/(mK). Chu pointed that the effect of varying zirconium contents on the microstructure affected the thermal conductivity of the Cu/diamond composites. The analysis suggested that the interfacial bonding can be effectively improved by the addition of minor amounts of zirconium.

Chung [20] used titanium as an additional element and prepared diamond/Cu-Ti composites by pressureless sintering method without impurities. The highest thermal conductivity was 608 W/(mK) when Ti was 2wt%. The XRD result shows that TiC was formed at a specific temperature of titanium and copper, and the TiC highly improved the thermal conductivity of the composite by improving the interfacial bonding of copper and diamond. All of the researches mentioned above can prove that additive element is effective of improving interfacial bonding and achieving good chemical affinity thus improving the thermal conductivity of composites.

2.3.2 Diamond surface metallization

Diamond surface metallization is improving the chemical affinity between matrix and diamond particles by coating the diamond surface with alloying elements. The coating on the diamond surface can react with diamond thus carbide layer can be formed after the reaction. This carbide layer is continuous, uniform, dense and the thickness can be controlled which can highly improve the interface. Compared to the metal matrix alloying method, the carbide layer obtained by coating on the diamond is much usable. The continuous interfacial layer can reduce the non-uniform nucleation or agglomeration of carbides and guarantee isotropic thermal conductivity, thus the composites have good thermal conductivity and mechanical properties in all directions.

Jin [21] prepared copper/diamond composites with tungsten coatings on diamond

particles prepared by the magnetron sputtering method and the copper/diamond composites were fabricated via pressureless infiltration. The lowest thermal resistance of the diamond-WC-copper interface was 3.75 $\times 10^{-8}$ (mK)/W. The researcher controlled the thickness of tungsten coating and the optimum thickness of the tungsten coating was 218nm, this thick coating can improve the densification of the composites and minimize the thermal boundary resistance.

Hai [22] fabricated copper-diamond composite materials with TiC coatings on diamond particles via electrodeposition. The researcher concluded that diamond particles with a size on the order of 400μm were successfully incorporated in a copper matrix via electrodeposition. The maximum thermal conductivity for composite with uncoated diamond particles was 454 W/(mK) when the diamond was 55vol%, the thermal conductivity of composite with TiC coated diamond particles was 471 W/(mK) when the diamond was 49vol%, an increase of thermal conductivity could be observed. However, the plating conditions for the incorporation of electrically conductive particles need to be operated carefully in the process, and using the lowest current density is attributed to the quality of the interfaces.

Qi [23] prepared copper/diamond composites with chromium carbide coatings on diamond particles via vacuum pressure infiltration. The as-fabricated composites, with Cr_7C_3 coatings formed on diamond particles, exhibit a thermal conductivity of 562 W/(mK). The Cr_7C_3 intermediate coatings effectively improved the interfacial bonding and decrease the interfacial thermal resistance of copper/diamond composites.

Qi [12] prepared copper/diamond composites with tungsten carbide coating on diamond particles via vacuum pressure infiltration. The WC coating was formed on the diamond particle surface via the molten salt method with WO_3 served as the medium. The thermal conductivity of the as-fabricated composite achieved 658

W/(mK). Compared to the composite with uncoated diamond particles, the WC coating significantly improved the interfacial bonding and thermal conductivity.

Li [24] fabricated graphite flakes/6063Al composites with SiC coatings on graphite flakes. The SiC coatings were prepared via the SiO_2 sol-gel method combining with in-situ reaction, the SiC coated graphite flakes /6063Al composites were fabricated by vacuum hot pressing. The highest thermal conductivity was 731.4 W/(mK), and the result showed that the SiC coating with a thickness of 15nm on the graphite flakes can effectively improve the chemical affinity and interfacial bonding, thus improving the thermal conductivity.

Chen [25] fabricated graphite flakes/copper composites via spark plasma sintering. Nickel was coated on graphite flakes through the electroless deposition. The highest thermal conductivity of Ni-coated graphite flakes/copper composite in X-Y direction was 532 W/(mK), the interfacial bonding between graphite flakes and copper matrix can be significantly improved by introducing electroless Ni-plating on graphite flakes and the hard Ni plating layer can also reduce internal cracking during preparation, thus the mechanical properties of the composite can be improved.

2.4 Fabrication methods

2.4.1 Vacuum hot pressing (VHP)

Vacuum hot pressing can be used for fabricating composites with high densification. The process is shown in Figure 2-4. The main processing is pressing and heats the powder compact in a graphite mold in a vacuum atmosphere, the desired high temperature and high pressure with a relatively long holding time (compared to spark plasma sintering) can make a chemical reaction happen between additional carbide forming element particles and diamond particles, then the product can combine with copper so the chemical affinity can be improved.

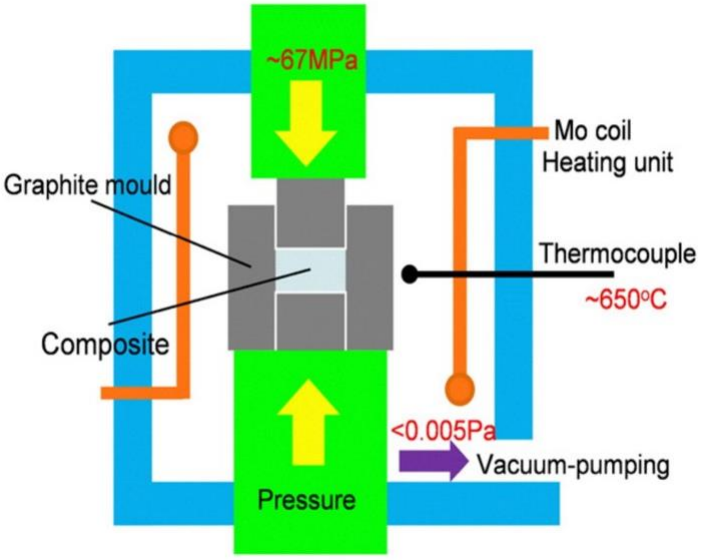

Figure 2-4 Schematic diagram of vacuum hot pressing process [26]

Han [27] successfully used this VHP to produce graphite film/copper composites at 1150 °C under the pressure of 1 MPa. The graphite flakes were uniformly dispersed in the copper matrix for the fabricated composite, and the composite had a low CTE of 2.18×10^{-5} K^{-1}, a high TC of 485.2 W/(mK).

Liu [28] used VHP to produce graphite/copper composites at a sintering pressure of 40MPa and a sintering temperature of 980 °C, and composite achieved a high thermal conductivity of 612W/(mK).

Zhao [16] used vacuum hot pressing to produce graphite flakes/copper composites at a sintering temperature of 1020°C and a sintering pressure 40MPa, and the thermal conductivity of the fabricated composite achieved 634.87 W/(mK).

2.4.2 Spark plasma sintering (SPS)

The spark plasma sintering (SPS) method, as shown in Figure 2-5, is one kind of

powder metallurgy. The composite powders are loaded into a graphite mold, and lower punch and the high pulse direct current are applied with desired pressure to sinter the powder. After discharge activation, the pores are discharged, a material with high performance can be acquired. SPS has the characteristics of sintering during pressurization. The plasma generated by the pulse current and the pressure during the sintering process is beneficial to reduce the sintering temperature of the powder. At the same time, the characteristics of low voltage and high current can make the powder fast sintered and dense. Spark plasma sintering has the advantages of fast heat speed and short sintering time. It can be used for low temperature and high pressure (500-1000MPa) sintering or low pressure and high temperature (1273-2273K) sintering, which is beneficial to control the structure of the sintered body and obtain highly densified samples.

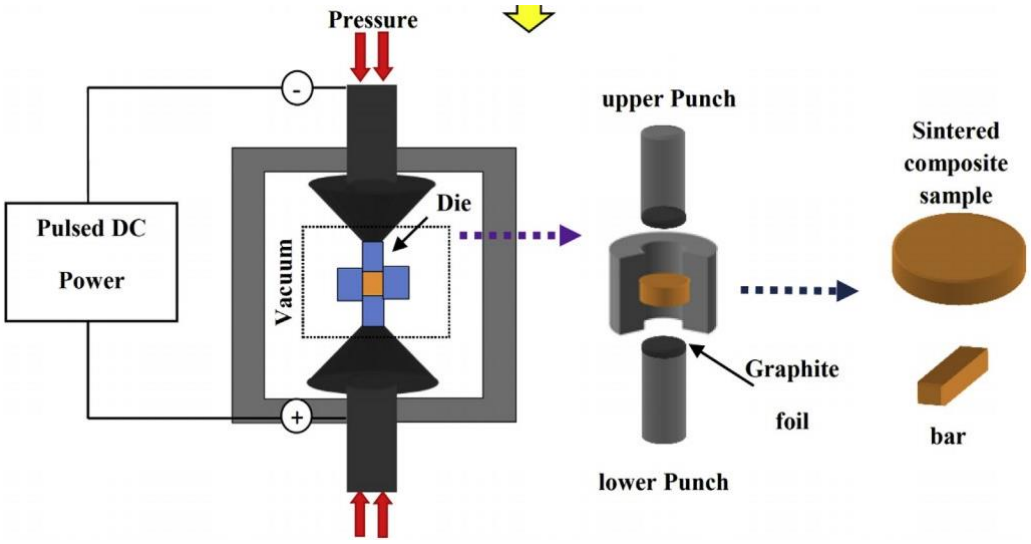

Figure 2-5 Schematic diagram of spark plasma sintering [29]

Tian [30] used SPS to fabricate the graphene oxide nanosheets-reinforced copper composites, and the fabricated composite has a high hardness, with a value of 411HV.

Ukhina [31] fabricated copper/diamond composites with W-containing coatings and copper/diamond composites with Ni-containing coatings by spark plasma sintering at a sintering temperature of 920°C for 3mins with a pressure 40MPa. His team concluded that copper/diamond composites with W-containing coatings on the diamond have better interfaces than the copper/diamond composites with Ni-containing coatings.

Zhou [32] investigated the effect of doping amount of copper-coated graphene on the tungsten-copper composites by SPS in an argon atmosphere with the temperature of 1150°C for 10mins under the pressure of 30MPa. When the doping of copper-coated graphene was 0.45wt%, the hardness of the composite was 238HV.

2.4.3 Electrodeposition

Electrodeposition is the oxidation of the anode metal which happens at the anode to form a suitable oxide film, this can be called electrochemical oxidation of metal or electrooxidation of metal. The process happens because current flows through the migration of positive and negative ions in the electrolyte solution under the action of an external electric field, and the redox reaction of gain and loss of electrons occurs on the electrode to form a coating. For copper/diamond composites, the electrodes are usually placed horizontally in the electrochemical solutions, diamond particles are first precipitated on the cathode substrate, and then copper is electrodeposited on the substrate to fill the gap between the precipitated diamond particles. The process of electrodeposition is shown in Figure 2-6.

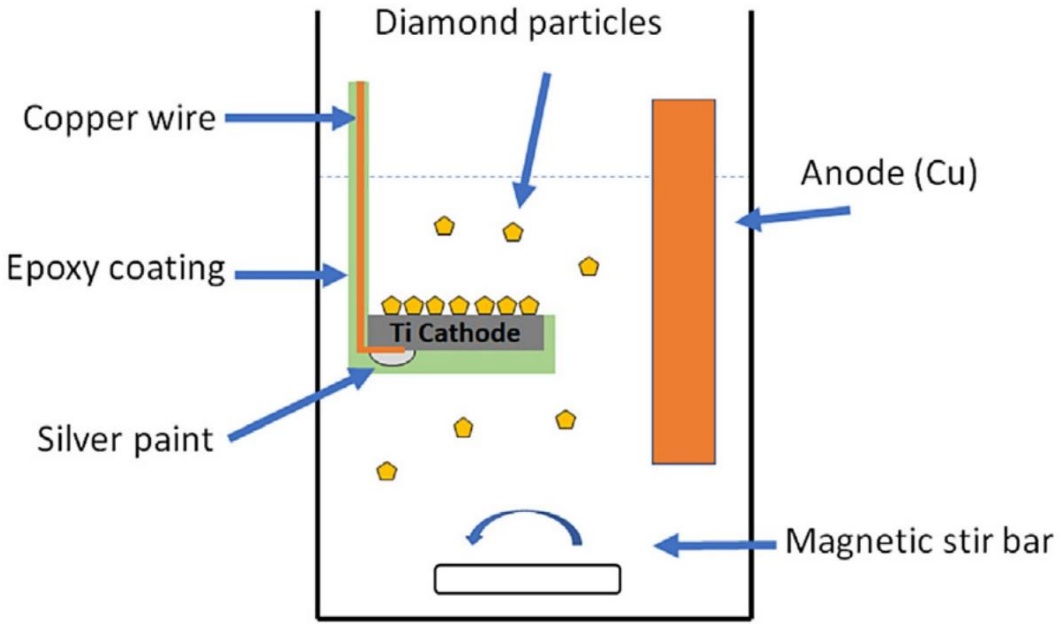

Figure 2-6 Schematic diagram of electrodeposition [22]

Wei [5] fabricated graphene/copper matrix composite foils by pulse electrodeposition and indicated that the tensile strength of Gr/Cu composite foil decreased from 367 up to 236 MPa, then increased up to 274 MPa with the increase of Gr contents from 0.04 up to 1.6 g/L in the electrolyte. This variation of tensile strength is caused by a non-monotonic change of graphene defects density in Gr/Cu composite foils partially.

Hagio [33] successfully prepared and adopted to fabricate copper/diamond composite plating by electrodeposition. Electrodeposition was carried out in a copper sulfate bath containing dispersed SiC-coated diamond. Copper was found to be directly deposited on the surface of SiC-coated diamonds in contrast to the pristine diamonds. The nanosized diamonds/copper composite plating containing 1.07wt% of SiC-coated nanosized diamonds showed a higher thermal conductivity of 46W/(mK).

Haijun [22] successfully incorporated diamond particles in the copper matrix using electrodeposition. They chose TiC coated diamond particles and uncoated diamond

particles as a comparison. The maximum thermal conductivity was 471W/(mK) at 49vol% of the diamond which is 17W/(mK) higher than uncoated diamond particles.

2.4.4 Powder hot forging

The forging process (as shown in Figure 2-7) performed above the metal recrystallization temperature is called hot forging. The process is (1) preparing the powders first; (2) mixing the powders in a V-type mixer at a specific speed for a specific time; (3) compacting the mixed powder at room temperature in the mold; and (4) forging at high temperature in atmosphere protective chamber (oxygen content less than 200ppm). Compared to other fabrication methods, powder forging can rapidly and cost-effectively prepare powder composites without expensive manufacturing equipment, and it offers an alternative and more effective method to fabricated metal matrix composites [34].

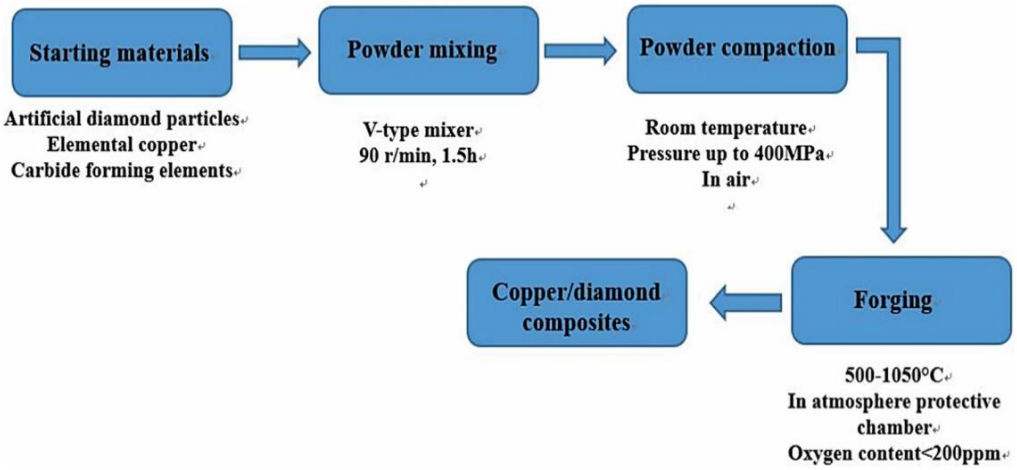

Figure 2-7 Schematic diagram of hot forging [35]

Our research group has used the powder hot forging technique to successfully fabricate copper/diamond composites from powders and investigate the carbide interface layer formation and influence on the resultant fabricated composites. The

primary findings are summarized as below:

Copper/Ti-coated diamond composites were successfully fabricated by hot forging at 800°C [36]. The result shows that hot forging can improve the density of the composite and the in-situ formation of TiC interface between copper matrix and diamond is helpful to form strong interfacial bonding which can improve thermal conductivity.

Copper/B-coated diamond composites were fabricated with different B content by hot forging at 1050°C [37]. It indicated that B_4C can be formed and B_4C interface can improve thermal conductivity, the highest thermal conductivity he achieved was 440W/(mK).

Copper/Ti-coated diamond composites were hot forged at 800°C and 1050°C [38]. It is found that the TiC coverage rate of composite forged at 800°C (96%) is higher than composite forged at 1050°C (70%). The hot forging temperature affects the formation of the carbide layer.

2.5 Summary and Research objectives

In summary, copper has relatively high thermal conductivity, good mechanical properties, and a wide range of usability. Diamond has excellent thermophysical properties and extremely high stiffness and strength; graphite flakes can be used as heat sink materials and thermal insulation materials at the same time due to its excellent thermophysical properties along the plane and extremely low thermal conductivity perpendicular to the slice direction, and it is also cost-effective. Therefore, copper/diamond composites and copper/graphite flakes composites are suitable for use as heat sink materials. However, both diamond particles and graphite flakes have a poor chemical affinity with the copper matrix, which leads to poor interfacial bonding. Especially for graphite flakes, the smooth surface of graphite flakes is difficult to form a mechanical bond with copper. The interface

performance is a key factor in determining the performance of composite materials, which can be improved by metal matrix alloying, diamond surface metallization, and controlling fabrication process, thus, the properties of the composites can be improved.

Our research group fabricated copper/diamond composites via hot forging, this method is easy to operate and cost-effective. We successfully prepared copper/55vol%diamond composites with thermal conductivity of 550 W/(mK), which is higher than most other composites fabricated via the same processing. This study uses surface metallization for Cu/diamond composites and metal matrix alloying for Cu/graphite flakes composites to improve the interfacial bonding strength and the mechanical properties of the composites, this study will focus on:

1) Fabricating Cu/diamond composites by vacuum sintering at 550℃, 650℃, 750℃ and 800℃, respectively. Investigating the effects of vacuum sintering on copper/tungsten coated-diamond composites at varying temperatures and analyzing the tungsten carbide formation mechanism.
2) Varying the volume fraction of the tungsten-coated diamond from 40 to 50%, to investigate the effects of volume fraction of tungsten-coated diamond particles on thermophysical properties of the fabricated copper/diamond composites.
3) Exploring the feasibility of fabrication of graphite flakes-reinforced copper composites by powder forging technique, and investigate the volume fraction of graphite flakes on the fabricated composite's properties.

3 Experimental Procedure

This chapter mainly describes raw materials information and specific methods and equipment used for material preparation, characterization, and testing. All of the composites are wire cut and the microstructure of the bulk and the extracted diamond particles are characterized by scanning electronic microscopy (SEM), and the phase constitution of all composites are analyzed by X-ray diffraction (XRD).

3.1 Materials Preparation

3.1.1 Raw Materials

3.1.1.1 Copper

The pure copper powders (having a purity of 99.7%, and size <45 μm) were supplied by Aldrich Company, NZ. The copper powders were used as the matrix.

3.1.1.2 Diamond particles

The M8D8 diamond powder (high-quality synthetic diamond powder) was coated with tungsten on the diamond surface, the diameter of the coated-diamond particles was 70-80 μm, having an octagonal shape, was supplied by Henan Huanghe Whirlwind Co., China.

3.1.1.3 Graphite flakes

The natural graphite flakes (99% carbon basis, +50 mesh particles size) were supplied by Sigma Aldrich Company, NZ.

3.1.2 Cleaning of raw materials

To remove the impurities and dust, the diamond particles were firstly rinsed in distilled water twice and then dried up in the oven which had been preheated at 80 °C for an hour. After that, the diamond particles were ultrasonic vibration cleaned for 20 minutes twice in the alcohol bath.

3.2 Manufacturing Process

3.2.1 Mixing of raw materials

The diamond particles and copper powder for Cu/diamond composites were mixed in a V-type mixer (Jiangyin Rongde Machinery) at speed of 60rpm for 90minutes. The graphite flakes and copper powder for Cu/Graphite flakes composites were mixed in a V- type mixer (Jiangyin Rongde Machinery) at speed of 60rpm for 90minutes.

3.2.2 Compaction

The powder mixture was pressed into a compact, with a diameter of 30mm and a height of 40mm at room temperature under a uniaxial pressure of 60MPa using a 100ton-hydraulic mechanical press. Then the pressing plunger was naturally released, and the compact was taken out.

3.2.3 Vacuum sintering

The compact was put in a ceramic tray, then the ceramic tray was placed on the plate in the vacuum sintering furnace. The door of the chamber was closed in a cater-cornered way. Then the process was set up as instructed. After finishing the process, the compact was cooled in the furnace to room temperature, and the compact was taken out.

3.2.4 Hot forging

The compact was placed in a steel mold and heated up to the desired temperature, and then forged. The whole process should be operated in an argon atmosphere (with an oxygen content of less than 200ppm).

All of the fabricated Cu/55vol% diamond composites are listed in Table 3-1, the fabricated Cu/graphite flakes composites are listed in Table 3-2.

Table 3-1 Fabricated copper/Diamond composites

Sample	**Size (Diameter/height) (mm/mm)**	**Fabrication process**	
		Vacuum sintering (°C/hour)	**Powder compact Hot forging temperature (°C)**
Cu/55W-Dia	30/40	800/2	1050
Cu/55W-Dia	30/40	-	1050
Cu/45W-Dia	10/17	-	1050
Cu/55W-Dia	10/17	-	1050
Cu/65W-Dia	10/17	-	1050
Cu/55W-Dia	10/17	800/1	-
Cu/55W-Dia	10/17	800/0.5	-
Cu/55W-Dia	10/17	750/1	-
Cu/55W-Dia	10/17	750/0.5	-
Cu/55W-Dia	10/17	650/0.5	-
Cu/55W-Dia	10/17	550/0.5	-

Table 3-2 Fabricated copper/Graphite flakes composites

Matrix	Volume fraction of GFs	Mass fraction of additive Ti element	Size (Diameter/ height) (mm/mm)	Powder compact Hot forging temperature (°C)
Cu	30	1.5	30/40	1050
Cu	40	1.5	30/40	1050
Cu	50	1.5	30/40	1050
Cu	60	1.5	30/40	1050
Cu	70	1.5	30/40	1050
Cu	50	1.5	30/40	950

3.3 Property testing

3.3.1 Density

The density of Cu/diamond composites and Cu/Graphite flakes composites were measured through Archimedes' principle. Each sample needs to be measured at least five times, and finally, the average will be taken. The mass and volume of samples were measured following the Archimedes principle, which is accurate and easy to operate.

The calculation formula is:

$$\rho = m_1/(m_1-m_2)\ \rho_{water}$$

ρ- density of the sample to be measured; m_1 - mass of the sample in the air; m_2 - mass of the sample in the water; $\rho_{water} = 1 g/cm^3$

3.3.2 Microstructure

Scanning Electron Microscope (SEM, HITACHI, s4700), as shown in Figure 3-1,

was used to characterize the micromorphology of the Cu/diamond composite bulks and Cu/Graphite flakes composites, and the extracted diamond particles and graphite flakes. Platinum needed to be coated on the surface of the samples firstly before SEM works to ensure a bright field of vision.

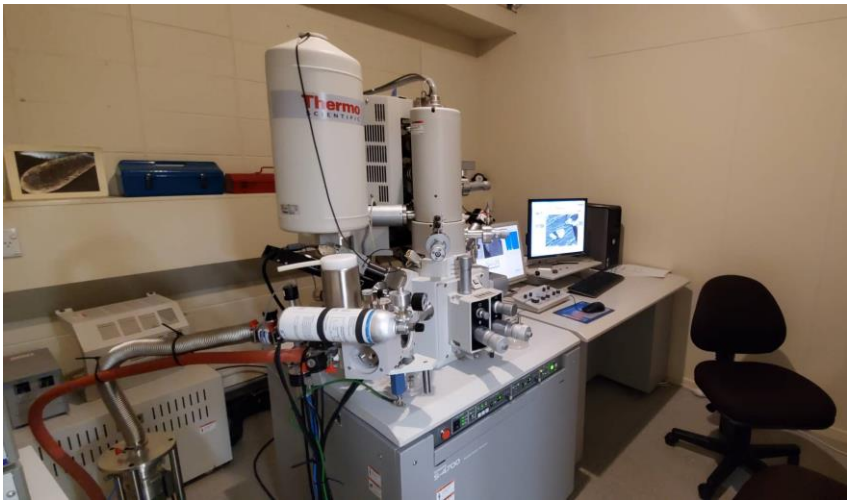

Figure 3-1 Image of SEM, HITACHI, s4700.

3.3.3 Phase constitution

Figure 3-2 Image of XRD, Philips

The phase constitution of Cu/diamond composites and Cu/Graphite flakes composites were determined by X-ray diffraction (XRD), equipped with Philips (The Netherlands Advanced X-ray), as shown in Figure 3-2. It can accurately

measure the intensity of different phases in the samples.

3.3.4 Thermal diffusivity

The thermal diffusivity of Cu/diamond composites and Cu/Graphite flakes composites were measured through laser flash technique, via LFA 467 equipment (Netzsch, Germany). The measurement is required to be operated at room temperature with the international standard dimension of Φ12.7 mm × 3 mm for the 30mm-diameter specimen and Φ10 mm × 2 mm for the 9mm-diameter sample. All of the Cu/diamond composites and Cu/Graphite flakes composites were required to be polished with water abrasive paper with 320 #, 1000 # and 2000 #, and followed by washed by distilled water and then ethanol ultrasonically washed for 3 minutes.

3.3.5 Thermal conductivity

The thermal conductivity of Cu/diamond composites and Cu/Graphite flakes composites were calculated via diffusivity by:

$$\lambda = \alpha \times \rho \times Cp \qquad \text{Equation 3-1}$$

λ (W/mK) - thermal conductivity of the composites; α (m2 /s) - thermal diffusivity; ρ (kg/m^3) - density of the composite and Cp (J/kg/K) - specific heat capacity of the composites.

4 Cu/diamond composites

4.1 Effect of vacuum sintering on Cu/diamond composites

To investigate the effect of vacuum sintering processing on the interface of W-coated copper/diamond composites, the listed samples in Table 4-1 were fabricated.

Table 4-1 Composites to investigate the effect of vacuum sintering on Cu/diamond composites

Samples	**Compositions**	**Size Diameter/height (mm/mm)**	**Fabrication process**	
			Vacuum sintering (°C/h)	**Hot forging (°C)**
Cu-55WDia-VS800C2h-1050HF	Cu/55vol%W-Diamond	30/40	800/2	1050
Cu-55WDia-1050HF	Cu/55vol%W-Diamond	30/40	-	1050
Cu-55WDia-VS800C2h	Cu/55vol%W-Diamond	30/40	800/2	-

4.1.1 Relative density

Figure 4-1 shows the measured relative density of Cu-55WDia-VS800C2h-1050HF composite, Cu-55WDia-VS800C2h composite, and Cu-55WDia-1050HF composite. It can see that the relative density of Cu-55WDia-VS800C2h-1050HF is 96.6%, which is much higher than the relative density of Cu-55WDia-1050HF which is 90.1%. The relative density of Cu-55WDia-VS800C2h is 83.5%. The

result shows the changing of fabrication processing can affect the relative density of composites, and the reason will be explained in the discussion section.

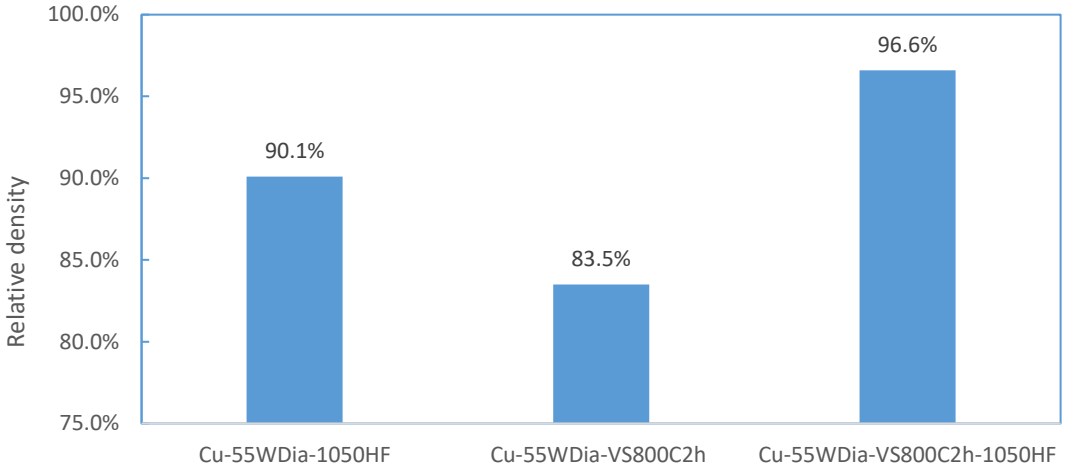

Figure 4-1 Relative density of Cu-55WDia-1050HF and Cu-55WDia-VS800/2h-1050HF

4.1.2 Phase constitutions

The X-ray diffraction patterns of Cu-55WDia-VS800C2h, Cu-55WDia-VS800C2h-1050HF, and Cu-55WDia-1050HF can be seen from Figure 4-2. For Cu-55WDia-VS800C2h, the diffraction of Cu, diamond, W_2C, and WC can be observed. For Cu-55WDia-VS800C2h-1050HF, the diffraction of Cu, diamond, W_2C, and WC can be observed. For Cu-55WDia-1050HF, the diffraction of Cu, diamond, W_2C, and WC can be observed.

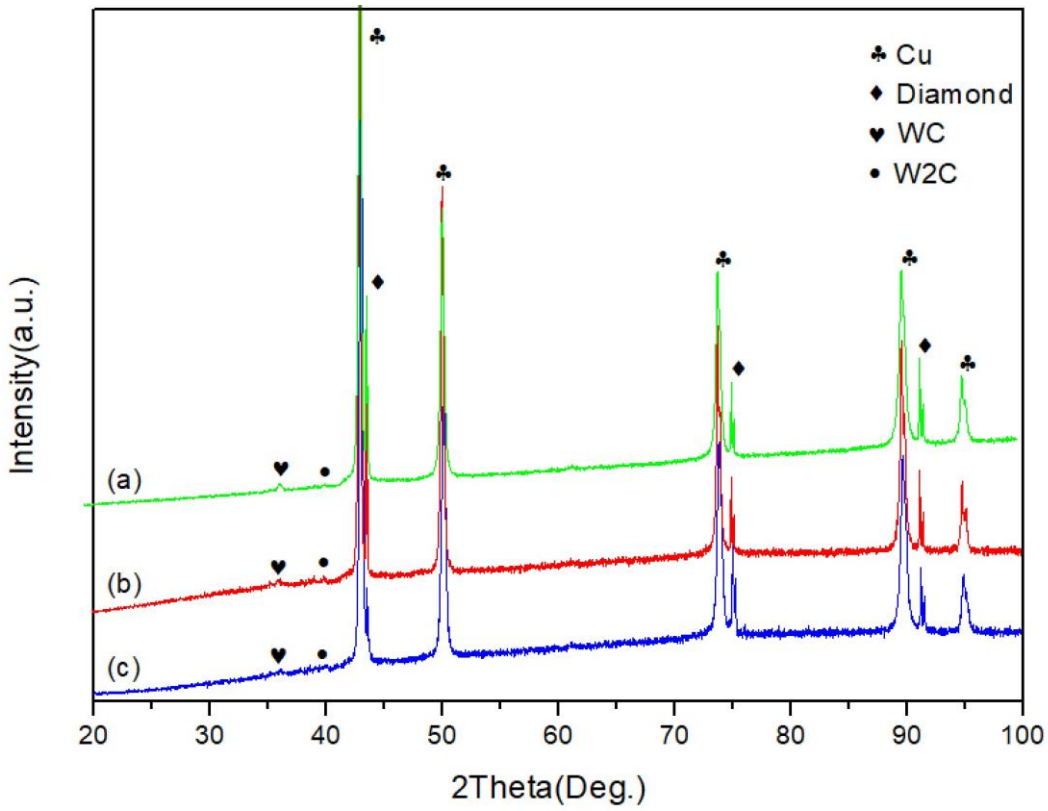

Figure 4-2 Phase constitution of: (a) Cu-55WDia-VS800C2h, (b) Cu-55WDia-VS800C2h-1050HF, and (c) Cu-55WDia-1050HF

The appearance of WC and W_2C can prove that W-coating reacted with diamond during both the vacuum sintering process and the hot forging process on the diamond surface.

The reaction mechanism is as following:

$$2W+C(Diamond)=W_2C \qquad \text{Equation 4-1}$$

$$W_2C+C(Diamond)=2WC \qquad \text{Equation 4-2}$$

W_2C is always formed firstly [39] and WC is much more stable than W_2C.

For Cu-55WDia-VS800/2h, the diffraction peaks of copper, diamond, W_2C, and WC can be seen, and the intensity of WC is strong. Thus, WC is the main composition of the interface for Cu-55WDia-VS800C2h composite. However, the content of W_2C is too small that the peak of W_2C is low. From the mechanism of tungsten carbide formation described in Equation 4-1 and Equation 4-2, it is known

that W_2C is always formed firstly. Therefore, the WC in Cu-55WDia-VS800C2h is generated via 2W+C(Diamond)=W_2C, W_2C+C(Diamond)=2WC.

For Cu-55WDia-VS800C2h-1050HF composite, the diffraction peaks of copper, diamond, W_2C and WC can be detected. The intensity of WC, and W_2C is almost the same, which points out that the interface of Cu-55WDia-VS800/2h-1050HF consists of WC and W_2C. Because of the two stages of the fabrication process, the WC is formed in two ways: (1) During the vacuum sintering process, W reacted with diamond to form W_2C firstly. Then W_2C further reacted with diamond to form WC. During the vacuum sintering process, W_2C and WC have been formed. (2) During the hot forging process, the W_2C formed during the vacuum sintering process can continuously react with diamond to form WC.

For Cu-55WDia- 1050HF, the diffraction peaks of copper, diamond, WC, and W_2C can be observed. The W-coating reacted with diamond to form W_2C, and the formed W_2C continued to react with diamond to form WC during the hot forging process. Thus, the interface of Cu-55WDia- 1050HF consists of W_2C and WC for Cu-55WDia-1050HF.

In both Cu-WDia-VS800C2h-1050HF and Cu-WDia-1050HF, from the XRD result, it can be expected that all of the tungsten coating has reacted with diamond to form W_2C and WC because the intensity of W cannot be detected.

4.1.3 Microstructure

Figure 4-3 shows the SEM images of Cu-WDia-VS800C2h-1050HF(a-c), and Cu-WDia-1050HF(d-e). For Cu-WDia-VS800C2h-1050HF, the dispersion of diamond in the copper matrix is evenly distributed. For Cu-WDia-1050HF, the dispersion of diamond is uniform. Some small pits can be observed in both Cu-WDia-VS800C2h-1050HF and Cu-WDia-1050HF (as the yellow arrows point in Figure

4-3(c) and Figure 4-3 (f)), it was reported as the graphitization of diamond [40], which is caused during sintering at 800°C and forging at 1050°C. However, a small gap (as marked by the red circles in Figure 4-3(a) and Figure 4-3 (d)) can be seen between diamond particles and copper matrix, which indicates that diamond particles and copper matrix have poor interfacial bonding in Cu-WDia-VS800C2h-1050HF and Cu-WDia-1050HF.

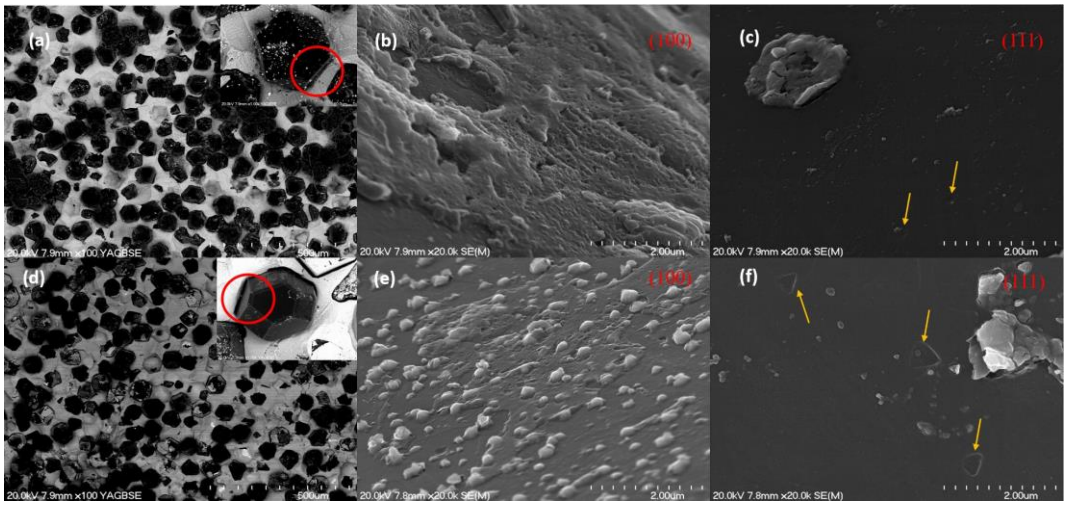

Figure 4-3 Microstructure of Cu-55WDia-VS800C2h-1050HF(a-c), and Cu-55WDia-1050HF(d-e)

In Cu-55W-Dia-VS800C2h-1050HF, the interface can be found on both diamond -{100}facet and -{111}facet, however, the interface is not continuous, can be seen from the high magnification images(Figure 4-3(b) and Figure 4-3(c)).

In Cu-55W-Dia-1050HF, the interface can be found on both diamond -{100}facet and -{111}facet, but the interface is not continuous, can be seen from high magnification images(Figure 4-3(e) and Figure 4-3(f)).

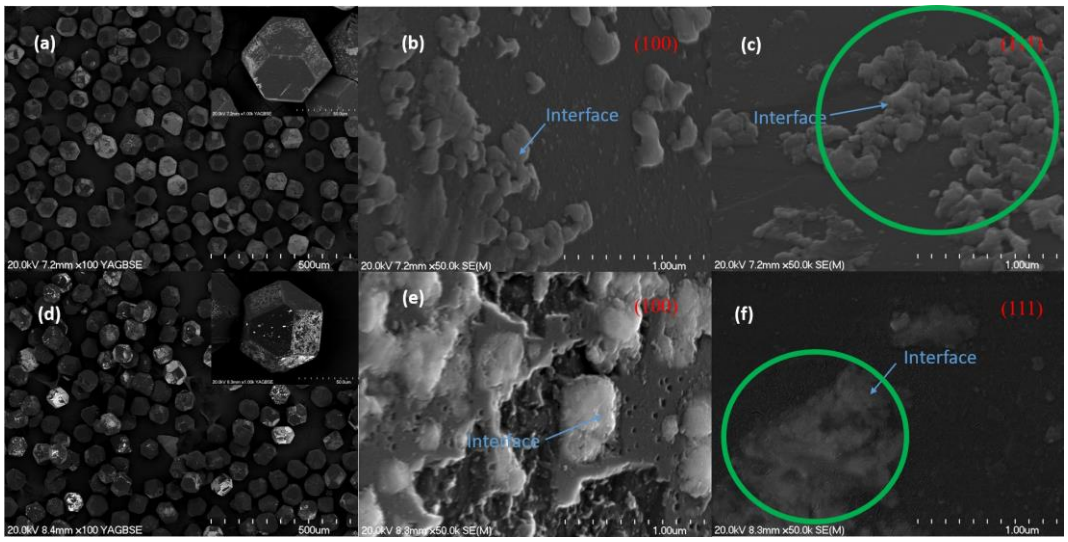

Figure 4-4 Extracted diamond particles from Cu-55WDia-VS800C2h-1050HF(a-c); Cu-55-Dia-1050HF(d-f).

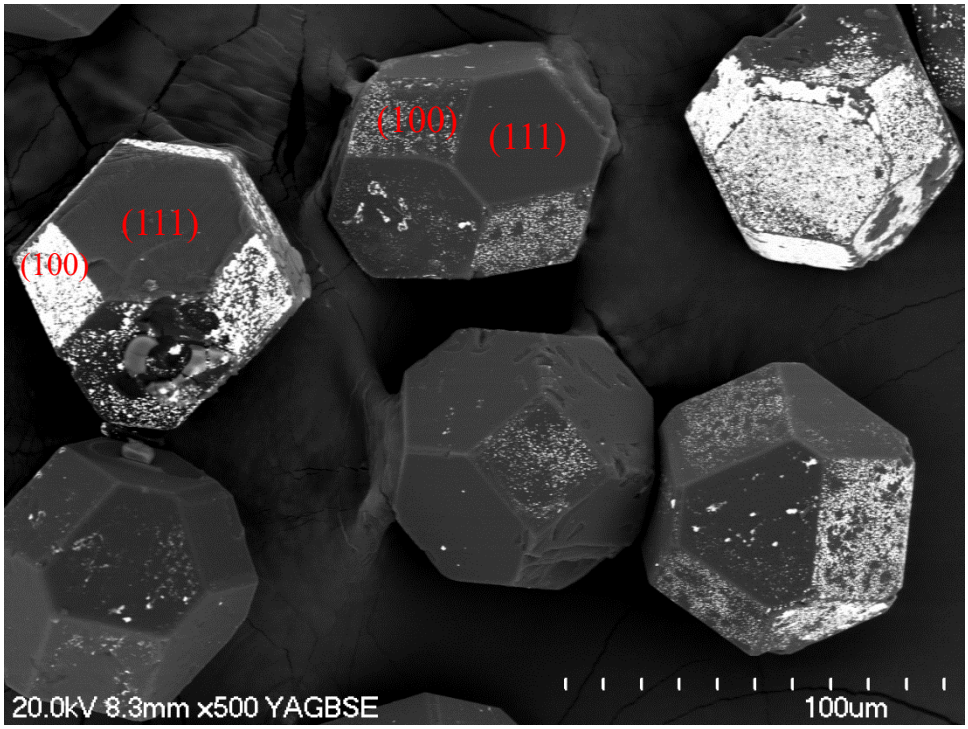

Figure 4-5 Extracted diamond particles of Cu-55WDia-1050HF

To further research the interface of the Cu-55WDia-VS800C2h-1050HF composite and Cu-55WDia-1050HF composite. Diamond particles were extracted from the Cu-55WDia-VS800C2h-1050HF and Cu-55WDia-1050HF composites and were characterized by SEM, as shown in Figure 4-4. The coverage rate for Cu-55WDia-

VS800C2h-1050HF composite is 14.3%, and the coverage rate for Cu-55WDia -1050HF composite is 24.1%. The coverage rate of extracted diamond of Cu-55WDia-VS800C2h was also be calculated, is 42.3%. The shedding of the interface on the diamond is similar among Cu-55WDia-VS800C2h-1050HF composite and Cu-55WDia-1050HF composite. Taking Cu-55WDia-1050HF as an example (as shown in Figure 4-5), the shedding of the interface on diamond -{111}facet is significantly more obvious than diamond -{100}facet. The interface on diamond -{100}facet is mostly reserved, however, the interface on diamond -{111}facet is mostly fall off.

The huge reduction of the coverage rate for Cu-55WDia-VS800C2h-1050HF after hot forging explains the formation of the interface, the interface formed during vacuum sintering was broken in the following hot forging process, which is attributed to spallation of WC interface that is brittle.

The surface of the diamond particles in Cu-55WDia-VS800C2h-1050HF composite and Cu-55WDia-1050HF composite is rough, and the discontinuous interface can be seen (as the blue arrows point out in Figure 4-4). It is clear to see that some of the diamond particles are covered by the interface (bright area in Figure 4-4).

For Cu-55WDia-VS800C2h-1050HF, the high coverage rate of diamond particles proves that the effective WC interface exists in abundance. The more interface on diamond particles means the better interfacial bonding between copper and diamond. For Cu-55WDia-VS800C2h-1050HF composite, the interface is discontinuous and the formation of the interface on diamond -{100}facet is more than diamond -{111}facet.

For Cu-55WDia -1050HF composite (as shown in Figure 4-4 (d-f)), the amount of interface (WC) on diamond -{100}facet is larger than that on the diamond -{111}facet. Most of the diamond -{100}facets are covered by interface, however,

the diamond -{111}facet has a little interface. The interface (WC) is not uniform and discontinuous.

4.1.4 Thermal conductivity

The thermal diffusivity and thermal conductivity of Cu-55WDia-VS800C2h-1050HF composite and Cu-55WDia -1050HF composite are shown in Figure 4-7. The thermal conductivity of Cu-55WDia-1050HF is 230.5W/(mK), which is higher than that of Cu-55WDia- VS800C2h-1050HF (317.7W/(mK)). This result agrees with the result of the coverage rate, which will be discussed later.

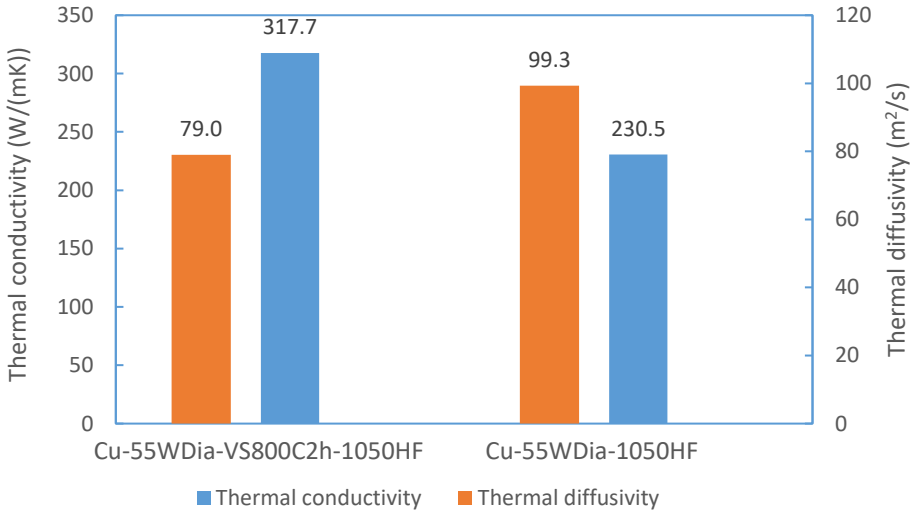

Figure 4-6 Thermal diffusivity and thermal conductivity of Cu-WDia-VS800C2h-1050HF, and Cu-W-Dia-1050HF

4.1.5 Discussion

4.1.5.1 Effect of vacuum sintering process on relative density and microstructure

The interface of the Cu/diamond composites affects the relative density and microstructure of Cu/diamond composites, vacuum sintering process can modify the interface, thus the vacuum sintering affects the relative density and

microstructure of Cu/diamond composites.

From the results mentioned above, the microstructure and phase constitutions of Cu-55WDia-VS800C2h-1050HF composite and Cu-55WDia -1050HF composite are almost the same, however, the relative density of Cu-55WDia-VS800C2h-1050HF composite (96.6%) is much higher than that of Cu-55WDia -1050HF composite (90.1%). The reason is that Cu-55WDia-VS800C2h-1050HF composite was fabricated in two stages, the fabrication process offered a longer time to form a larger amount of effective WC interface than Cu-55WDia -1050HF. The more interface formed, the better interfacial bonding between copper matrix and diamond particles, thus the higher relative density can be achieved.

Vacuum sintering has a significant effect on the diamond particles in different facets. Ruch [41] suggested that C atoms are bonded by two C-C bonds on the diamond -{100}facet, C atoms are bonded by three C-C bonds on the diamond -{111}facet. The surface energy of diamond -{111}and diamond -{100} facets are 5×10^{-5} J/cm2 and 8×10^{-5} J/cm2, respectively [8]. The diamond -{100}facet has higher surface energy, which means the diamond -{100}facet is unstable and the tungsten coating is easier to react with diamond -{100} than diamond -{111}facet. The Cu-55WDia-VS800C2h-1050HF composite has a similar microstructure with Cu-55WDia -1050HF composite, both of these two samples have more interface on diamond -{100}facet than diamond -{111}facet. Because of the low surface energy of the diamond -{111} facet, the atoms on the diamond -{111} facet are not as active as that on the diamond -{100} facet. Thus, the reaction of tungsten and diamond happened earlier on diamond -{100}facet than on diamond -{111}facet. The WC interface formed on diamond -{100}facet is more stable and has a larger amount than diamond -{111}facet.
The Cu-55WDia-VS800C2h-1050HF has a lower surface coverage rate than The Cu-55WDia-1050HF, but Cu-55WDia-VS800C2h-1050HF has a higher

relative density. The reason may be because the backscattering technique requires a strong contrast to distinguish copper, diamond, and interface, however, the contrast between fine WC particles and diamond is not strong when the image is at low magnification. Compare Figure 4-4(c) and Figure 4-4(f), partially continuous fine WC particles can be viewed (marked by the green circle) on Cu-55WDia-VS800C2h-1050HF. Thus, the WC has two kinds: one is fine WC particles, the other is rough WC particles. The fine WC particles have two possible formation routes: (1) the layer of fine WC particles was formed during 800℃ 2h vacuum sintering and bonded with diamond surface strongly that it was not broken during the following 1050℃ hot forging process; (2) the layer of fine WC was formed during the following 1050℃ hot forging process. From the high magnification SEM images of extracted diamond particles in Cu-55WDia -1050HF, the fine partially continuous WC particles cannot be observed, thus the formation of the fine WC particles has not happened during 1150 hot forging. It can be reasonably speculated that during the 800℃ 2h vacuum sintering process, the broken of the WC particles has not happened on the partially continuous thin layer of WC particles because of the strong bonding between WC and diamond.

4.1.5.2 Effect of vacuum sintering process on thermal conductivity

Modifying the interface for Cu/diamond composites is the method to improving the thermal conductivity of Cu/diamond composites, vacuum sintering process has a significant effect on the interface, thus vacuum sintering also affects thermal conductivity. 55WDia-VS800C2h-1050HF achieved a relatively higher thermal conductivity than 55WDia-1050HF. The reason is even if the rough WC particles were broken in the following hot forging process, the 55WDia-VS800C2h-1050HF still had a thin layer of partially discontinuous WC particles strongly bonded to diamond, the WC particles strongly bonded to diamond made a huge contribution to the thermal conductivity of 55WDia-VS800C2h-1050HF.

4.1.5.3 Effect of vacuum sintering on formation of interface

From the discussion mentioned above, vacuum sintering is helpful to form an effective interface and improve the relative density of Cu/diamond composites. However, the formed WC particles can be broken in the following hot forging process, thus optimizing the vacuum sintering conditions will be the solution. This will be discussed in the following part.

4.2 Effect of volume fraction of diamond particles on Cu/Dimond composites

To verify the suitable volume fraction of diamond particles in hot-forged Cu/diamond composites, three copper/diamond composites with diamond particles from 45vol% to 65vol% were investigated. The composite's composition and processing conditions are listed in Table 4-4.

Table 4-2 Composites to investigate the volume fraction of diamond

Samples	**Composition**	**Size Diameter/Height (mm/mm)**	**Fabrication process**
			Hot forging (°C)
Cu-45WDia-1050HF	Cu/45vol%W-Diamond	10/17	1050
Cu-55WDia-1050HF	Cu/55vol%W-Diamond	10/17	1050
Cu-65WDia-1050HF	Cu/65vol%W-Diamond	10/17	1050

4.2.1 Relative density

The relative density of Cu-45WDia-1050HF, Cu-55WDia-1050HF, and Cu-65WDia-1050HF is shown in Figure 4-10. The relative density of Cu-45WDia-1050HF is 99.2%, which is the highest among these three samples. The relative density is 89.5% for Cu-55WDia-1050HF, and 86.4% for Cu-65WDia-1050HF. It can be seen that with increasing the volume fraction of W-diamond, the relative density of the Cu/diamond composite is decreased. Yang [42] reported that diamond agglomerations were observed when the diamond particles were at a 55% volume fraction. This is because diamond particles are difficultly deformed in the hot forging process, the movement of diamond particles is limited during forging, thus the agglomeration of diamond particles happens.

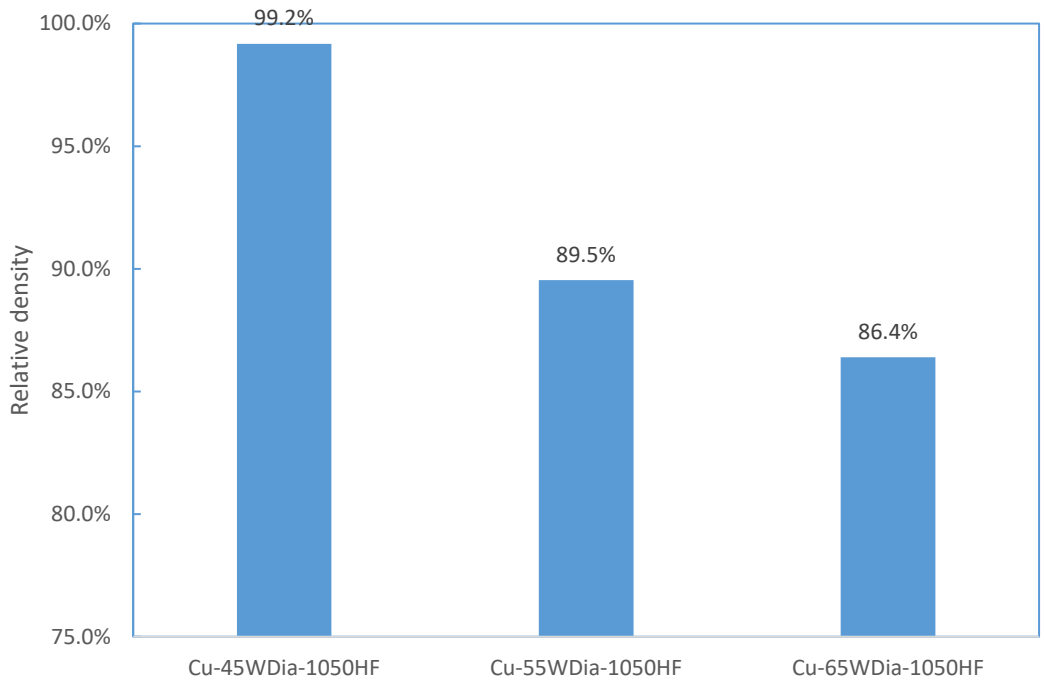

Figure 4-7 Relative density of Cu-45WDia-1050HF, Cu-55WDia-1050HF, and Cu-65WDia-1050HF

4.2.2 Phase constitutions

The phase constitutions of Cu-45WDia-1050HF, Cu-55WDia-1050HF, and Cu-

65WDia-1050HF are shown in Figure 4-11. For Cu-65WDia-1050HF composite, the phase of WC can be determined, the appearance of WC proves that the reaction between W-coating and diamond happened during the 1050°C hot forging process. For Cu-55WDia-1050HF, the phase of WC can also be determined, the same as Cu-65WDia-1050HF. However, the intensity of WC in Cu-55WDia-1050HF is lower than the intensity of WC in Cu-65WDia-1050HF. For Cu-45WDia-1050HF, the phase of WC cannot be observed, the reason may be the volume fraction of W-coated diamond particles is too small that after the reactions $2W+C(Diamond)=W_2C$ and $W_2C+C(Diamond)=2WC$ happening, the intensity of the formed WC particles was too weak to determine.

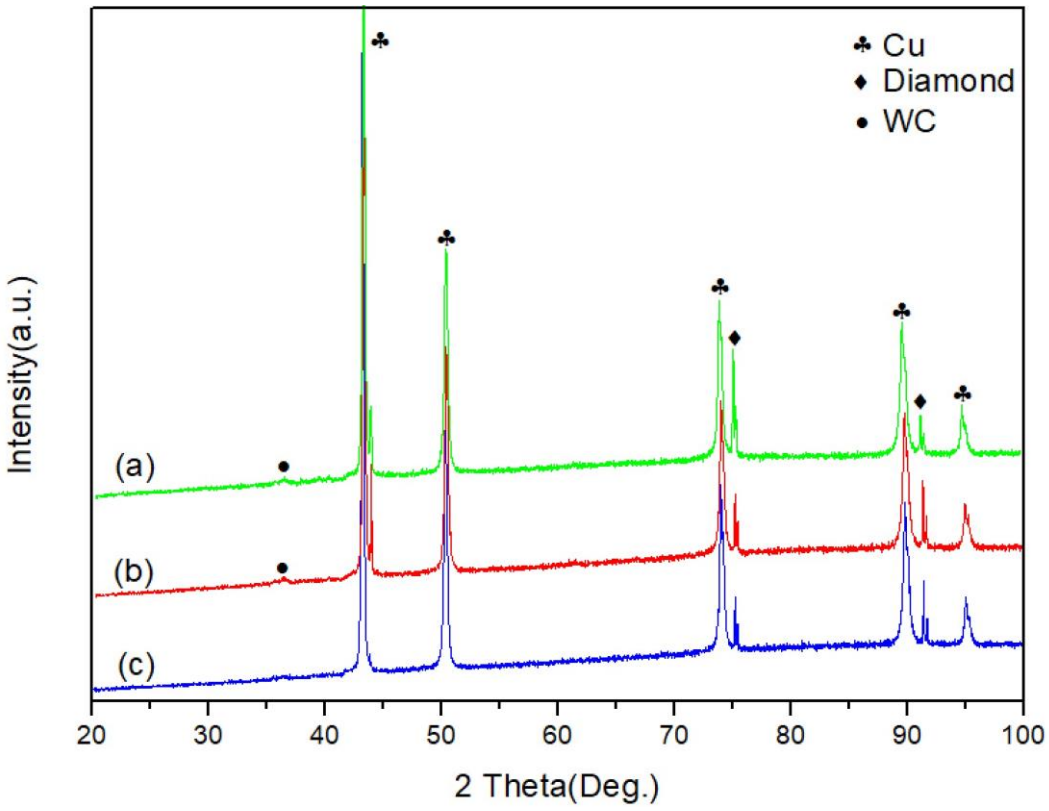

Figure 4-8 The phase constitution of: (a)Cu-65WDia-1050HF, (b)Cu-55WDia-1050HF, and (c)Cu-45WDia-1050HF

4.2.3 Microstructure

The morphology of Cu-45WDia-1050HF, Cu-55WDia-1050HF, and Cu-65WDia-1050HF composite bulks is shown in Figure 4-12. It can be seen that some small particles are on the surface of both diamond -{100} facet and diamond -{111} facet. These are the formed discontinuous interface. From the high magnification morphology images Fig.4-12 (b)-(e)-(h) and (c)-(f)-(i), it can see that the formed WC interface is increasing with the volume fraction of the W-diamond particles increased. The gaps (as marked in Figure 4-12 (a)(d)(g) by the red circles) between copper and diamond particles can also be observed. Besides, the agglomeration of diamond particles can be observed in Cu-65WDia-1050HF, it is consistent with the literature [42]. Yang [42] reported that when the volume fraction of diamond particles was 55%, diamond particles agglomerate in Cu/diamond composite.

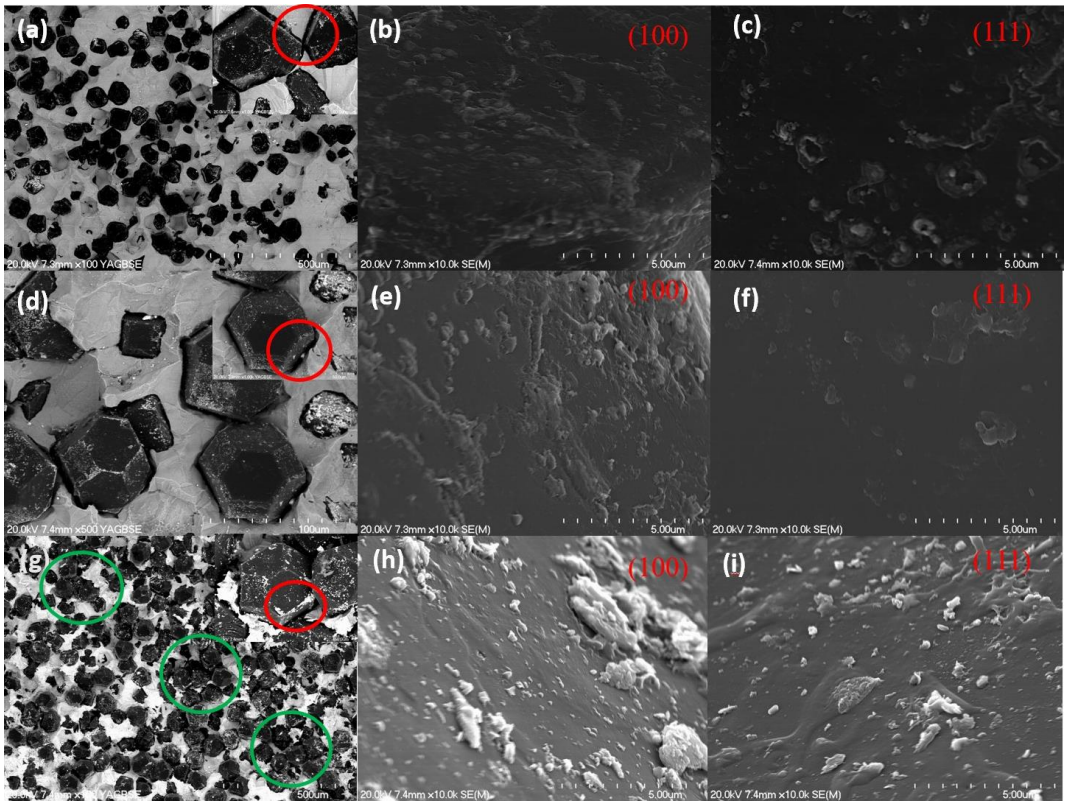

Figure 4-9 Microstructure of (a-c) Cu-45WDia-1050HF, (d-e) Cu-55WDia-1050HF, and (g)-(i) Cu-65WDia-1050HF

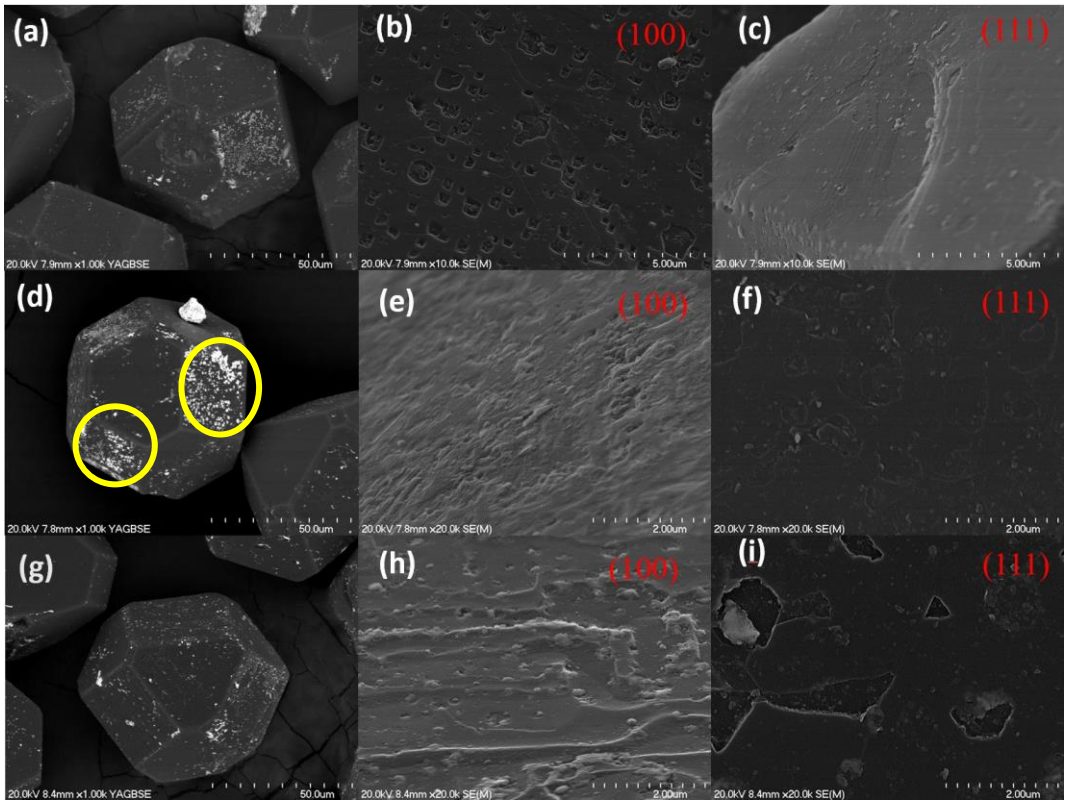

Figure 4-10 Microstructure of the extracted diamond particles from (a-c) Cu-45WDia-1050HF, (d-e) Cu-55WDia-1050HF, and (g)-(i) Cu-65WDia-1050HF composites

To further explore the character of the interface between copper and diamond, the diamond particles were extracted from Cu-45WDia-1050HF, Cu-55WDia-1050HF, and Cu-65WDia-1050HF composites. The morphology of the extracted diamond particles is shown in Figure 4-13. The coverage rate for Cu-45WDia-1050HF is 7.34%, the coverage rate for Cu-55WDia-1050HF is 18.7%, and the coverage rate for Cu-65WDia-1050HF is 10.87%. The surface of the diamond particles is rough after the 1050°C hot forging process, the small pits formed because of the graphitization of diamond can also be observed [40].

4.2.4 Thermal conductivity

The diffusivity and thermal conductivity of Cu-45WDia-1050HF, Cu-55WDia-1050HF, and Cu-65WDia-1050HF composites are shown in Figure 4-14. The Cu-

45WDia-1050HF composite has the highest thermal conductivity among these three composites, which is 250.8W/(mK). The thermal conductivity of Cu-55WDia-1050HF is 138.6W/(mK). The Cu-65WDia-1050HF composite has the lowest thermal conductivity of 65.1W/(mK).

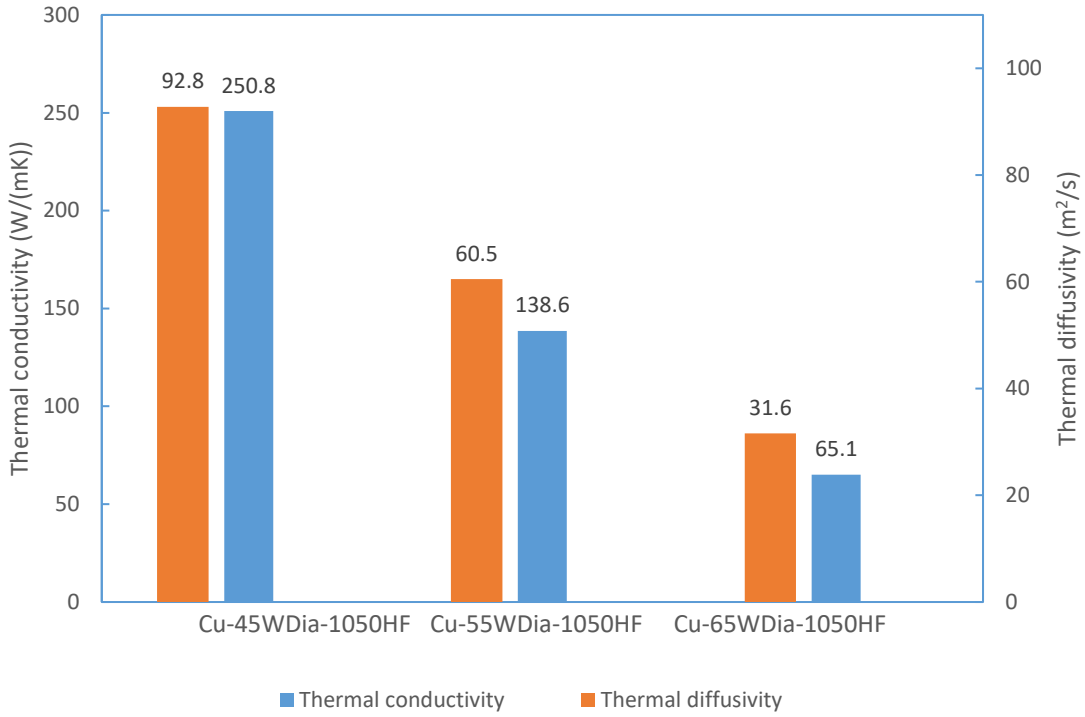

Figure 4-11 Thermal diffusivity and thermal conductivity of Cu-45WDia-1050HF, Cu-55WDia-1050HF, and Cu-65WDia-1050HF composites

4.2.5 Discussion

4.2.5.1 Effect of the volume fraction of diamond particles on relative density and microstructure

From the data of the relative density of Cu-45WDia-1050HF, Cu-55WDia-1050HF, and Cu-65WDia-1050HF, it can be concluded that with the volume fraction of diamond particles increasing from 45% to 65%, the relative density of Cu/diamond composites decreases from 99.2% to 86.4%. The highest coverage rate is 18.7% of Cu-55WDia-1050HF, however, the Cu-55WDia-

1050HF has a low relative density. The huge reduction of relative density may due to the agglomeration of diamond particles. From the information mentioned above in section 4.1.5, diamond particles agglomerate when the volume fraction of diamond particles at 55%, it can be viewed from Figure 4-12(g) when the volume fraction of diamond particles is at 65%, the phenomenon of the diamond agglomeration (as marked by the green circles) also exists, which is similar to Cu-55 vol.%diamond-1 vol.%Ti composites [42] fabricated by Fei. The distribution of diamond particles in Cu-55 vol.%diamond-1 vol.%Ti composites is inhomogeneous and diamond particles agglomerate [42]. The diamond particles stack together when the volume fraction of diamond particles was 55% and 65%, the dispersion of the diamond particles was not uniform, thus the relative density was low.

For the microstructure, as shown in Figure 4-13(a)(d)(g), diamond -{100}facet has more interface than diamond -{111}facet in Cu-45WDia-1050HF, Cu-55WDia-1050HF, and Cu-65WDia-1050HF. However, it can be observed that Cu-55WDia-1050HF has the biggest and brightest area (as marked by the yellow circles) among these three composites, which correspond to the coverage rate. The surface of the diamond particles is not flat, and the small pits caused by the graphitization of the diamond particles during the 1050℃ hot forging process can be observed. The microstructure of Cu-45WDia-1050HF, Cu-55WDia-1050HF, and Cu-65WDia-1050HF has no significant difference.

4.2.5.2 Effect of volume fraction of diamond particles on thermal conductivity

For Cu-45WDia-1050HF composite, it has the highest thermal conductivity among these three samples, the reasons may be: (1) the dispersion of diamond particles was not uniform, the diamond particles are stacked together when the volume fraction of diamond particles at 55% and 65%, thus the bonding

between diamond and copper is not strong in the diamond stacking area, and it causes low thermal conductivity in the diamond stacking area; (2) the formed interface with strong interface bonding with both copper matrix and diamond particles facilitate the phonon transfer from the copper to the diamond[38], however, with the volume fraction of the diamond particles increasing, the contact boundary between diamond and copper increases, the scattering of phonons increases, thus the thermal conductivity decreases.

4.3 Summary

This chapter illustrates the effect of the vacuum sintering process and the effect of the volume fraction of diamond particles on diamond/Cu composites.

(1) The reaction between W-coating and diamond particles happened during vacuum sintering above 550°C and with a sintering time > 30mins.
(2) The reaction between W-coating and diamond particles also happened when the sample was hot forged at 1050°C, and the reaction can be observed more intense on diamond -{100} facet than diamond -{111} facet.
(3) For Cu-55WDia-VS800/2h-1050HF composite, WC formed during vacuum sintering was partially broken during hot forging because of the brittleness property of WC ceramic material.
(4) With the volume fraction of diamond particles increasing from 45vol% to 65%, the relative density of Cu/diamond composites decrease from 99.2% to 86.4%, and the thermal conductivity of Cu/diamond particles decrease from 250.8W/(mK) to 62.1W/(mK).

5 Cu/Graphite flakes composites

To investigate the feasibility of graphite flakes reinforced copper matrix fabricated by powder hot forging and effects of additive titanium powders on the interface of copper/graphite flakes composites, graphite flakes/copper composites with graphite flakes volume fraction from 30vol% to 70vol% and 1.5wt% of Ti addition were fabricated, and the samples' preparation conditions are listed in Table 5-1.

The processing of Cu/graphite flakes composites is shown in Figure 5-1. The cold pressing direction and forging direction are along Z direction. Since graphite flakes are anisotropy, after the cold pressing and the hot forging process, the graphite flakes will arrange along the direction perpendicular to the applying pressure, which is X-Y direction. The microstructure of Cu/graphite flakes composites cross-section discussed later is along Z direction. The thermal conductivity of Cu/graphite flakes composites has been tested both along Z direction and X-Y direction.

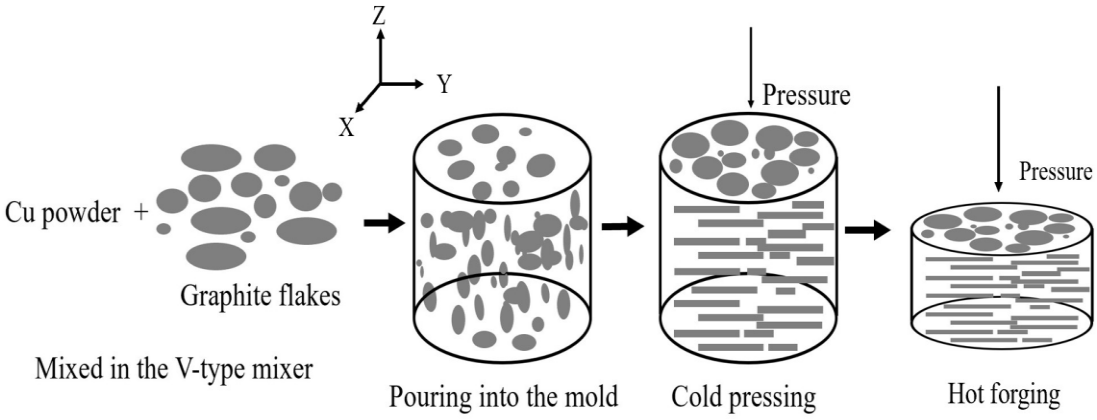

Figure 5-1 The processing of fabricating the Cu/graphite flakes composites

Table 5-1 Cu/graphite flakes composites

Samples	**Compositions**	**Size Diameter/ height (mm/mm)**	**Fabrication process**
			Hot forging (°C)
Cu-Ti-30GFs-1050HF	Cu/30vol% Graphite flakes mixed with Ti1.5wt% powder	10/17	1050
Cu-Ti-40GFs-1050HF	Cu/40vol% Graphite flakes mixed with Ti1.5wt% powder	10/17	1050
Cu-Ti-50GFs-1050HF	Cu/50vol% Graphite flakes mixed with Ti1.5wt% powder	10/17	1050
Cu-Ti-60GFs-1050HF	Cu/60vol% Graphite flakes mixed with Ti1.5wt% powder	10/17	1050
Cu-Ti-70GFs-1050HF	Cu/70vol% Graphite flakes mixed with Ti1.5wt% powder	10/17	1050
Cu-Ti-0GFs-950HF	Cu/50vol% Graphite flakes mixed with Ti1.5wt% powder	10/17	950

5.1 Relative density

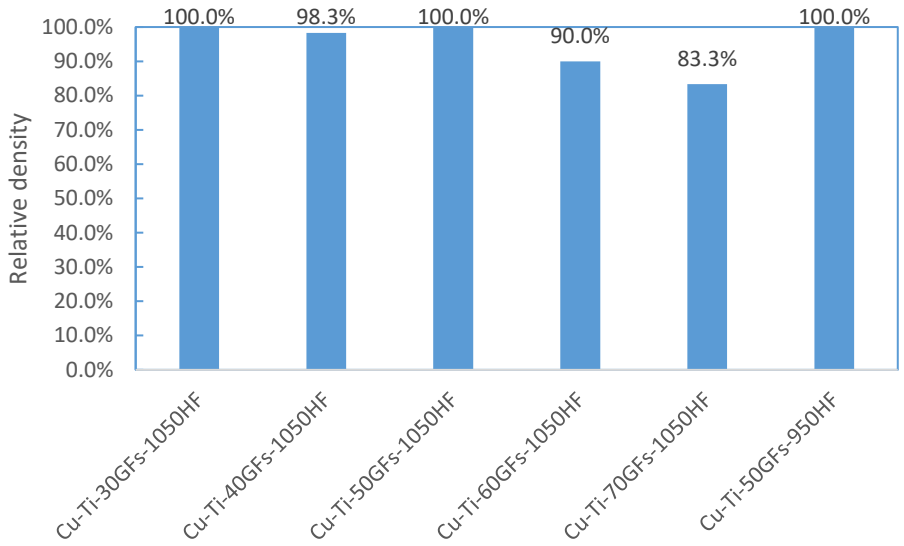

Figure 5-2 Relative density of Cu/Graphite flakes composites

Figure 5-2 reveals the relative density of Cu-Ti-30to70GFs-1050HF and Cu-Ti-50GFs-950HF. It can see that Cu-Ti-30to50GFs-1050HF and Cu-Ti-50GFs-950HF are fully dense. However, for Cu-Ti-60GFs-1050HF and Cu-Ti-70GFs-1050HF, the relative density respectively is only 89.9% and 83.3%.

5.2 Phase constitutions

The X-ray diffraction patterns of Cu-Ti-30to70GFs-1050HF and Cu-Ti-50GFs-950HF are shown in Figure 5-3. It can be seen that a significant amount of TiC can be detected in Cu-Ti-30GFs-1050HF, Cu-Ti-40GFs-1050HF, and Cu-Ti-50GFs-1050HF, which means the addition of 1.5wt% Ti powder reacted with graphite flakes during the 1050°C hot forging process to form TiC. For Cu-Ti-60GFs-1050HF and Cu-Ti-70GFs-1050HF composites, the intensity of TiC is too weak to detect. Among all of the samples, the intensity of TiC of Cu-Ti-40GFs-1050HF is significantly strong, it can be speculated that 40% of the volume fraction of graphite flakes is the critical volume fraction of Cu/graphite flakes composites.

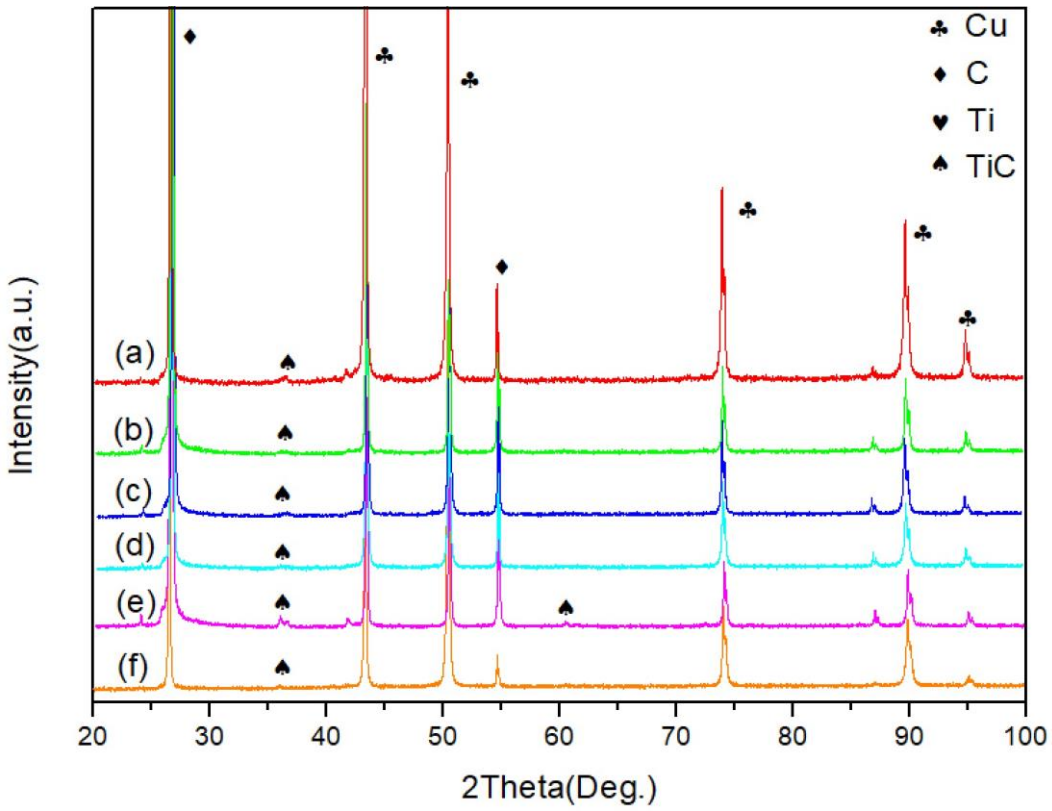

Figure 5-3 The X-ray diffraction patterns of: (a)Cu-Ti-50GFs-950HF, (b)Cu-Ti-70GFs-1050HF, (c)Cu-Ti-60GFs-1050HF, (d)Cu-Ti-50GFs-1050HF, (e)Cu-Ti-40GFs-1050HF, and (f)Cu-Ti-30GFs-1050HF

5.3 Microstructure

The microstructure images of Cu-Ti-50GFs-1050HF and Cu-Ti-50GFs-950HF are shown in Figure 5-4. The cross section shown in Figure 5-5(a)(e) is along Z direction, corresponding to Figure 5-1. The bright region represents the Cu, while the elongated dark region represents the graphite flakes. It can be seen that graphite flakes are homogeneously arranged, and the distribution of graphite flakes in the Cu matrix is nearly parallel. In the process of hot forging, the graphite flakes are arranged automatically perpendicular to the direction of applied pressure. Moreover, irregular particles can be seen in the Cu matrix (marked by red arrows). In addition, graphite flakes are affected by the surrounding Cu matrix in the hot forging process and some layers of graphite flakes might be bent. From Figure 5-4(b) and Figure 5-4(f), the gaps between copper and graphite flakes can be seen, the agglomerated

TiC exist between copper and graphite flakes.

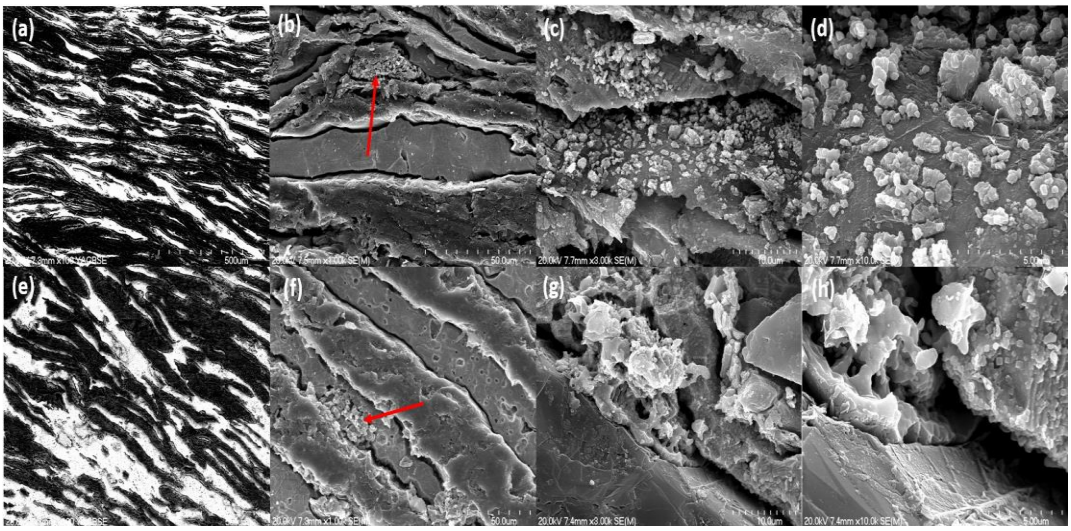

Figure 5-4 Microstructure of Cu-Ti-50GFs-1050HF(a)-(d); Cu-Ti-50GFs-950HF(e)-(h) in the direction parallel to stress

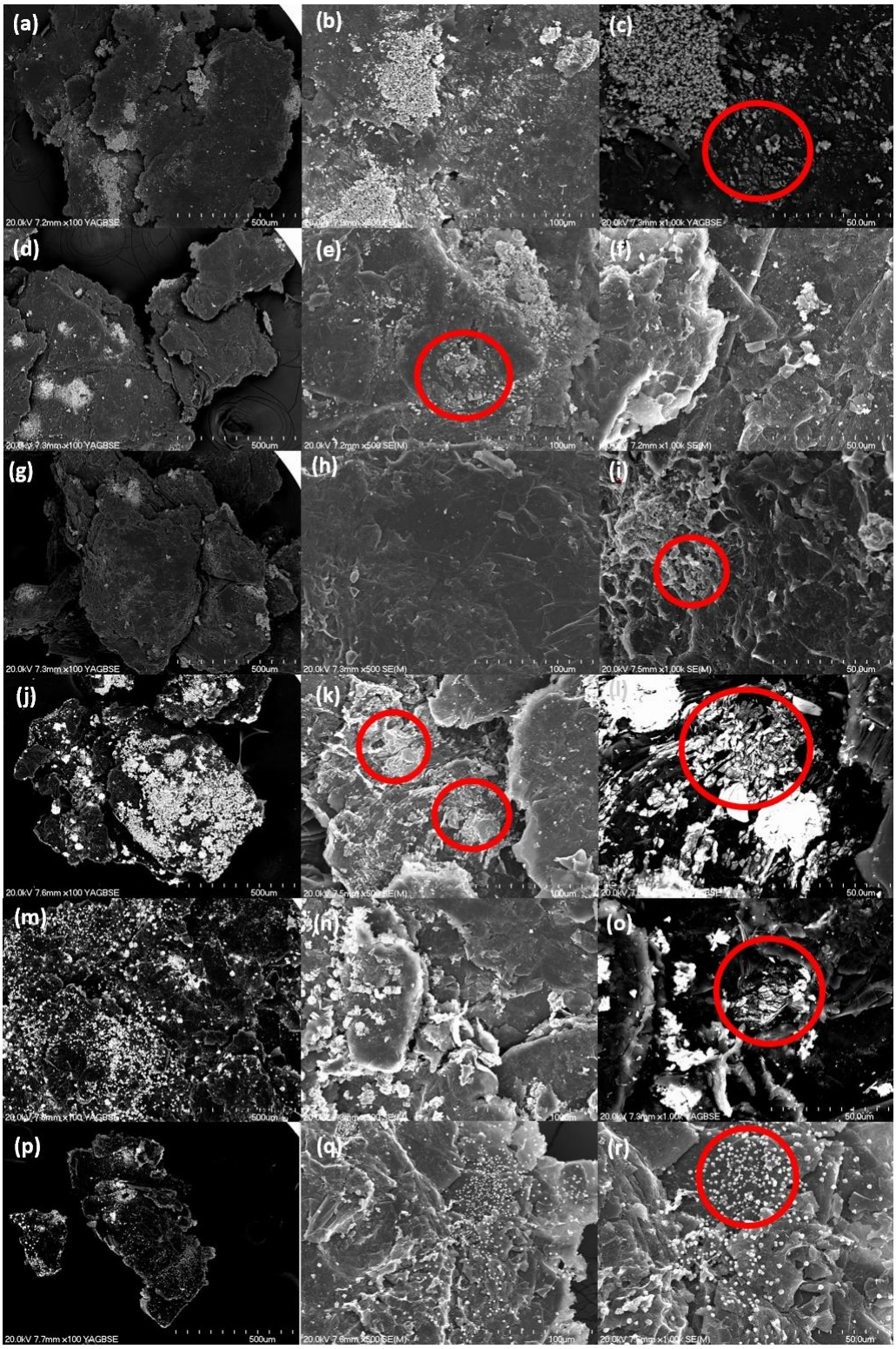

Figure 5-5 Microstructure of the extracted graphite flakes of Cu-Ti-30GFs-1050HF(a)-(c), Cu-Ti-40GFs-1050HF(d)-(f), Cu-Ti-50GFs-1050HF(g)-(i), Cu-Ti-60GFs-1050HF(j)-(l), Cu-Ti-70GFs-1050HF(m)-(o), and Cu-Ti-50GFs-950HF(p)-(r)

To further investigate the interface microstructure of Cu/ graphite flakes composites,

the graphite flakes were extracted from the composites, analyzed by SEM, and the morphology of corresponding diamond particles are presented in Figure 5-5. For Cu-Ti-30to70GFs-1050HF, the surface of the graphite flakes was rough, and discontinuous TiC particles can be observed. Figure 5-5(e) and Figure 5-5(k) clearly show the layer structure of graphite flakes. All of these five composites have partial river rippled TiC (circled by the red circles) on graphite flakes' surfaces. It suggests that the addition of 1.5wt% Ti powders is not enough to form a continuous TiC interface layer that fully covers the surface of graphite flakes. With the increase of volume fraction of graphite flakes, the formed effective TiC interface layer decreases, which can see from the changes in Figure 5-5(b)-(e)-(h)-(k)-(n).

5.4 Thermal conductivity

The thermal properties of Cu-Ti-50GFs-950HF Z, Cu-Ti-50GFs-950HF X-Y, and Cu-Ti-50GFs-1050HF X-Y have been tested (assume the direction perpendicular to the applied pressure is X-Y, the direction parallel to the applied pressure is Z), as shown in Figure 5-6. The diffusivity of Cu-Ti-50GFs-1050HF along X-Y direction is 82.1 m^2/s, the thermal conductivity of Cu-Ti-50GFs-1050HF along X-Y direction is 202.7 W/(mK). The diffusivity of Cu-Ti-50GFs-950HF along X-Y direction is 150.2 m^2/s and the thermal conductivity of Cu-Ti-50GFs-950HF along X-Y direction is 375.0 W/(mK). The diffusivity of Cu-Ti-50GFs-950HF along Z direction is 24.5 m^2/s, the thermal conductivity along the Z direction is 61.3 W/(mK). The result corresponds to the anisotropic properties of graphite flakes, that graphite flakes have high thermal conductivity in-plane and low thermal conductivity out-of-plane.

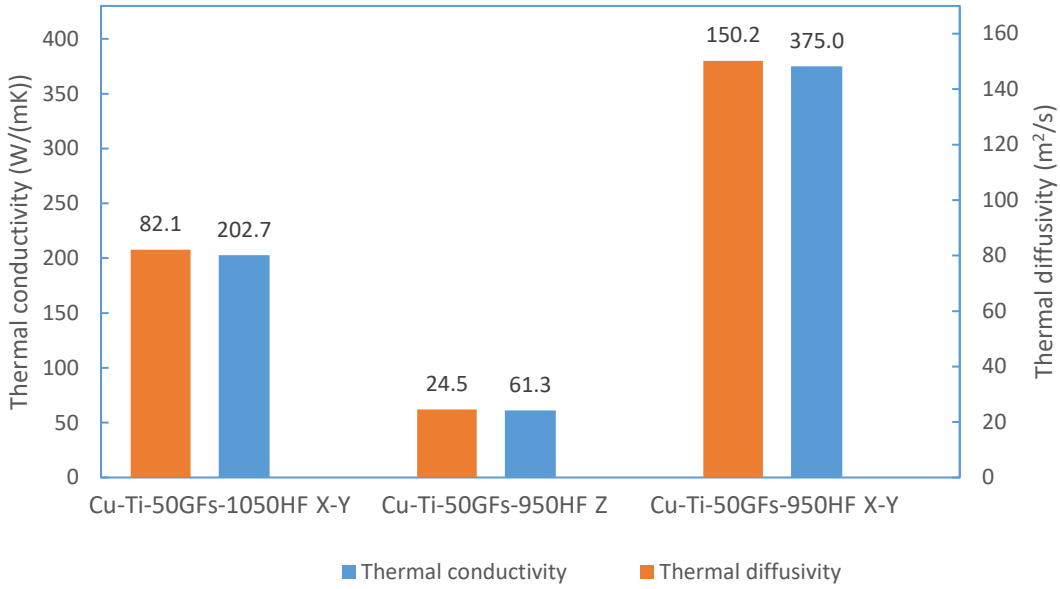

Figure 5-6 Thermal conductivity of Cu-Ti-50GFs-950HF along the direction to the applying force and Cu-Ti-50GFs-950HF along the direction perpendicular to the applying force

5.5 Discussion

5.5.1 Effect of volume fraction of graphite flakes

From the relative density results, it can be seen that Cu-Ti-30GFs-1050HF, Cu-Ti-40GFs-1050HF, Cu-Ti-50GFs-1050HF, and Cu-Ti-50GFs-950HF were fully sintered. This is because copper is ductile, plastic deformation happens during the hot forging process, and the viscosity of graphite flakes is high, thus copper and graphite flakes combined well. However, the relative density of Cu-Ti-60GFs-1050HF and Cu-Ti-70GFs-1050HF was low. The huge reduction of relative density may be because with the volume fraction of graphite flakes increasing, copper is less, graphite flakes are inclined to contact each other, the effective TiC cannot effectively improve the interfacial bonding between the contacting graphite flakes. The agglomeration of graphite flakes also happen, thus the relative density is low.

Combining the microstructure images in Figure 5-5, with the volume fraction of graphite flakes increasing from 30vol% to 70vol%, the discontinuous interface becomes more uneven, agglomeration of the TiC is more obvious. This is because with the volume fraction of graphite flakes increasing, the adding 1.5wt%Ti powder is not enough to fully cover the surface of graphite flakes, it causes some of the areas of the surface not covered by the effective interface, however, the other area is covered by formed TiC during hot forging. The Ti atoms are easy to diffuse to the area with Ti powder-covered during the hot forging process, thus agglomeration happens. Cu matrix to spread on rough graphite flakes during hot forging, thus filling the gaps and microvoids caused by the insufficient filling of Cu. The Cu-Ti-40GFs-1050HF has a significant intensity of TiC, which represents Cu/GFs composite with 40vol% graphite flakes has a more effective interface than the other samples. 50vol% of graphite flakes can be considered as the critical volume fraction because for Cu-Ti-60GFs-1050HF and Cu-Ti-70GFs-1050HF, the significant reduction of the relative density can be measured. However, Cu-Ti-50GFs-1050HF is fully dense, this implies for Cu/graphite flakes composites with volume fraction of graphite flakes above 50vol%, the components in the composites cannot be combined well.

5.5.2 The effect of hot forging temperature on thermal conductivity GFs/copper composites

By comparing the thermal conductivity results of Cu-Ti-50GFs composites hot forged at 950°C and 1050°C, the thermal conductivity of Cu-Ti-50GFs-1050HF respectively is and 202.7 W/(mK). It is much lower than the thermal conductivity of Cu-Ti-50GFs-950HF, which is 375.0 W/(mK). For Cu-Ti-50GFs-1050HF, the interface is discontinuous and some of the TiC particles agglomerated together (as shown in Figure 5-4(k) marked by the red circles) that the distribution of effective interface is not uniform. For Cu-Ti-50GFs-950HF, although the interface was not continuous, the TiC particles are

distributed relatively uniform, no significant agglomeration could be observed. Ren indicated that the temperature influences the extrusion of matrix copper [17], it was found that when the sintering temperature was above 1000°C, the extrusion of matrix copper was easy due to its low viscosity. However, when the fluidity of copper is too high, graphite flakes tend to agglomerate due to the difference in density between copper and graphite flakes.

For comparing the thermal conductivity of Cu-Ti-50GFs-1050HF and Cu-Ti-50GFs-950HF, the copper matrix in Cu-Ti-50GFs-1050HF fabricated at 1050°C had a higher fluidity than the copper matrix in Cu-Ti-50GFs-950HF, the agglomeration of graphite flakes happened in Cu-Ti-50GFs-1050HF, thus Cu-Ti-50GFs-1050HF has a lower thermal conductivity than Cu-Ti-50GFs-950HF.

5.5.3 The effect of Ti powder on interface of Cu/ graphite flakes composites

During the hot forging processing, Ti powder as a solid solute in Cu matrix first reacted with graphite flakes at the interface between graphite flakes and copper, then a Ti depleted region was formed near the interface. This concentration gradient of Ti element in the Cu matrix provides the driving force for their continuing migration into the Ti depleted region at the interface. Similar interface formation in the sintering process was reported by Ren[17]. Because of the addition of the Ti element, the formation of the interface helps to improve the thermal conductivity of Cu/ graphite flakes composites.

5.6 Summary

This chapter illustrates the interface and thermal conductivity of Cu-Ti-GFs composites with graphite flakes volume fraction changing from 30vol% to 70vol% fabricated by 1050°C hot forging and 950°C hot forging.

(1) The Cu-Ti-30to70GFs-1050HF and Cu-Ti-50GFs-950HF were successfully prepared by hot forging.

(2) The reaction of Ti powder and graphite flakes happened while the hot forging temperature is higher than 950°C.

(3) With the volume fraction of graphite flakes changing from 30vol% to 70vol%, the relative density of Cu/graphite flakes composites decreases from 100% to 83.3%.

(4) The thermal conductivity of Cu-Ti-50GFs-950HF along the X-Y direction was 375.0 W/(mK), the thermal conductivity of Cu-Ti-50GFs-1050HF along the X-Y direction was 202.7 W/(mK). This attributes to the strong interfacial bonding between the interface and the graphite flakes and the copper matrix, which improve the phonon transport in the composites. Controlling the reaction between Ti and graphite flakes can affect the TiC particles' nucleation and formation during hot forging. The thermal conductivity can be changed by adjusting the hot forging temperature.

(5) The hot forging temperature of 1050°C can lead the copper matrix to have an excessive-high fluidity, which can cause the agglomeration of graphite flakes. Thus, the thermal conductivity of Cu-Ti-50GFs-1050HF is lower than Cu-Ti-50GFs-950HF.

6 Conclusion

(1) Both vacuum sintering process and hot forging process are effective method to fabricate copper/diamond composites. However, the formed tungsten carbide during vacuum sintering can be broken in the following hot forging process because of the brittleness.

(2) WC can be formed on both diamond -{100}facet and -{111}facet during both vacuum sintering process and hot forging process, and it is easier for WC to formed on diamond -{100}facet than diamond -{111}facet.

(3) For copper/diamond composites, with the volume fraction of W-diamond increase from 45vol% to 65vol%, the relative density of the composite decreases from 99.17% to 86.4%, and the thermal conductivity of the composite decreases from 250.8 W/(mK) to 65.12W/(mK).

(4) The highest thermal conductivity of diamond/Cu composites was 250.8247 W/(mK) of Cu-45WDia-1050HF.

(5) Cu/ graphite flakes composites can successfully be fabricated via powder hot forging process at 950℃ and 1050℃.

(6) The Cu/graphite flakes composites can be fully dense after 1050℃ hot forging with a volume fraction of graphite flakes at 30vol%, 40vol%, and 50vol%. However, with the volume fraction of graphite flakes at 60vol% and 70vol%, the relative density drops significantly because agglomeration of graphite flakes happens and the dispersion of graphite flakes is not uniform.

(7) The highest thermal conductivity of the Cu/graphite flakes composites was 374.98 W/(mK) of Cu-Ti-50GFs-950HF along the X-Y direction.

Reference

1. Li, J., et al., *Optimized thermal properties in diamond particles reinforced copper-titanium matrix composites produced by gas pressure infiltration.* Composites Part A: Applied Science and Manufacturing, 2016. **91**: p. 189-194.
2. Wu, Y., et al., *Critical effect and enhanced thermal conductivity of Cu-diamond composites reinforced with various diamond prepared by composite electroplating.* Ceramics International, 2019. **45**(10): p. 13225-13234.
3. van Schilfgaarde, M., I.A. Abrikosov, and B. Johansson, *Origin of the Invar effect in iron–nickel alloys.* Nature, 1999. **400**(6739): p. 46-49.
4. Huang, F., et al., *The machinability of KOVAR material.* Journal of Materials Processing Technology, 1999. **87**(1-3): p. 112-118.
5. Wei, K.X., et al., *Mechanical behaviors of graphene/copper matrix composite foils fabricated by pulse electrodeposition.* Surfaces and Interfaces, 2021. **24**.
6. Zuo, T., et al., *Enhanced electrical conductivity and hardness of Copper/Carbon Nanotubes composite by tuning the interface structure.* Materials Letters, 2020. **280**.
7. Ankit, et al., *The effect of titanium carbide particles on microstructure and mechanical properties of copper/graphite composites prepared by flake powder metallurgy route.* Materials Today: Proceedings, 2020. **26**: p. 1140-1144.
8. Harkins, W.D., *Energy Relations of the Surface of Solids I. Surface Energy of the Diamond.* The Journal of Chemical Physics, 1942. **10**(5): p. 268-272.
9. Osipov, A.S., et al., *Diamond composites of high thermal conductivity and low dielectric loss tangent.* Materials Science and Engineering: B, 2021. **269**.
10. *Frontmatter*, in *Synthetic Diamond Films*. 2011. p. i-xxviii.
11. Xie, Z., et al., *Tailoring the thermal and mechanical properties of diamond/Cu composites by interface regulation of Cr alloying.* Diamond and Related Materials, 2021. **114**.
12. Kang, Q., et al., *Microstructure and thermal properties of copper–diamond composites with tungsten carbide coating on diamond particles.* Materials Characterization, 2015. **105**: p. 18-23.
13. Chen, L., Z. Yan, and S. Kumar, *Coupled electron-phonon transport and heat transfer pathways in graphene nanostructures.* Carbon, 2017. **123**: p. 525-535.
14. Zhang, X., N. Zhao, and C. He, *The superior mechanical and physical properties of nanocarbon reinforced bulk composites achieved by architecture design – A review.* Progress in Materials Science, 2020. **113**.
15. Liu, B., et al., *Effect of graphite flakes particle sizes on the microstructure and properties of graphite flakes/copper composites.* Journal of Alloys and Compounds, 2018. **766**: p. 382-390.
16. Zhao, Y., et al., *Effect of boron on the microstructure and properties of graphite flakes/copper composites fabricated by vacuum hot pressing.* Journal of Alloys and Compounds, 2020. **815**.
17. Ren, S., et al., *Effect of matrix-alloying-element chromium on the microstructure and properties of graphite flakes/copper composites fabricated by hot pressing sintering.* Carbon, 2018. **127**: p. 412-423.
18. Bai, G., et al., *High thermal conductivity of Cu-B/diamond composites prepared by gas pressure infiltration.* Journal of Alloys and Compounds, 2018. **735**: p. 1648-1653.

19. Chu, K., et al., *On the thermal conductivity of Cu–Zr/diamond composites.* Materials & Design, 2013. **45**: p. 36-42.
20. Chung, C.-Y., et al., *High thermal conductive diamond/Cu–Ti composites fabricated by pressureless sintering technique.* Applied Thermal Engineering, 2014. **69**(1-2): p. 208-213.
21. Jia, J., et al., *Enhanced thermal conductivity in diamond/copper composites with tungsten coatings on diamond particles prepared by magnetron sputtering method*. Materials Chemistry and Physics, 2020. **252**.
22. Cho, H.J., Y.-J. Kim, and U. Erb, *Thermal conductivity of copper-diamond composite materials produced by electrodeposition and the effect of TiC coatings on diamond particles.* Composites Part B: Engineering, 2018. **155**: p. 197-203.
23. Kang, Q., et al., *Preparation of copper–diamond composites with chromium carbide coatings on diamond particles for heat sink applications.* Applied Thermal Engineering, 2013. **60**(1-2): p. 423-429.
24. Li, T., et al., *Effect of nanometer SiC coating on thermal conductivity and bending strength of graphite flake/6063Al composites.* Journal of Alloys and Compounds, 2021. **862**.
25. Chen, J., et al., *Properties and microstructure of nickel-coated graphite flakes/copper composites fabricated by spark plasma sintering.* Carbon, 2017. **121**: p. 25-34.
26. Tan, Z., et al., *Diamond/aluminum composites processed by vacuum hot pressing: Microstructure characteristics and thermal properties.* Diamond and Related Materials, 2013. **31**: p. 1-5.
27. Han, X., et al., *Fabrication of graphite films/copper composites by vacuum hot pressing for high-efficiency thermal management property.* Composites Communications, 2021. **24**.
28. Liu, Q., et al., *Effects of morphological characteristics of graphite fillers on the thermal conductivity of the graphite/copper composites fabricated by vacuum hot pressing sintering.* Vacuum, 2019. **167**: p. 199-206.
29. sayyad, R., et al., *Preparation of Ag/reduced graphene oxide reinforced copper matrix composites through spark plasma sintering: An investigation of microstructure and mechanical properties.* Ceramics International, 2020. **46**(9): p. 13569-13579.
30. Tian, N., et al., *Microstructure and tribological properties of titanium matrix nanocomposites through powder metallurgy using graphene oxide nanosheets enhanced copper powders and spark plasma sintering.* Journal of Alloys and Compounds, 2021. **867**.
31. Ukhina, A., et al., *Morphological features of W- and Ni-containing coatings on diamond crystals and properties of diamond-copper composites obtained by Spark Plasma Sintering.* Materials Today: Proceedings, 2017. **4**(11): p. 11396-11401.
32. Zhou, K., et al., *W-Cu composites reinforced by copper coated graphene prepared using infiltration sintering and spark plasma sintering: A comparative study.* International Journal of Refractory Metals and Hard Materials, 2019. **82**: p. 91-99.
33. Hagio, T., et al., *Electrodeposition of nano-diamond/copper composite platings: Improved interfacial adhesion between diamond and copper via formation of silicon carbide on diamond surface.* Surface and Coatings Technology, 2020. **403**.
34. Yang, F., et al., *Effect of Minor Titanium Addition on Copper/Diamond Composites Prepared by Hot Forging.* Jom, 2018. **70**(10): p. 2243-2248.
35. Jia, S.Q. and F. Yang, *High thermal conductive copper/diamond composites: state of the art.* Journal of Materials Science, 2020. **56**(3): p. 2241-2274.

36. Ma, J.N., L. Bolzoni, and F. Yang, *Interface manipulation and its effects on the resultant thermal conductivity of hot-forged copper/Ti-coated diamond composites.* Journal of Alloys and Compounds, 2021. **868**.
37. Lei, L., L. Bolzoni, and F. Yang, *Interphase layer characteristics and thermal conductivity of hot-forged Cu-B/diamond composites.* Advanced Composites and Hybrid Materials, 2021.
38. Lei, L., L. Bolzoni, and F. Yang, *High thermal conductivity and strong interface bonding of a hot-forged Cu/Ti-coated-diamond composite.* Carbon, 2020. **168**: p. 553-563.
39. Zhang, C., et al., *Effects of dual-layer coatings on microstructure and thermal conductivity of diamond/Cu composites prepared by vacuum hot pressing.* Surface and Coatings Technology, 2015. **277**: p. 299-307.
40. Shao, W.Z., et al., *A study on graphitization of diamond in copper–diamond composite materials.* Materials Letters, 2004. **58**(1-2): p. 146-149.
41. Ruch, P.W., et al., *Selective interfacial bonding in Al(Si)–diamond composites and its effect on thermal conductivity.* Composites Science and Technology, 2006. **66**(15): p. 2677-2685.
42. Yang, F., et al., *Titanium-Doped Copper-Diamond Composites Fabricated by Hot-Forging of Powder Mixtures or Cold-Pressed Powder Preforms.* Jom, 2019. **71**(12): p. 4867-4871.